VARIAN ASSOCIATES

BEVERLY, MASSACHUSETTS

HYDROGEN MASER PROGRAM

INTERIM TECHNICAL REPORT

30 JANUARY 1964

PERIOD COVERED: 1 FEBRUARY 1962 TO 31 MAY 1963

THIS WORK IS SUPPORTED BY THE NATIONAL AERONAUTICS AND SPACE ADMINISTRATION UNDER CONTRACT NAS 8-2604.

Varian Associates
Beverly, Mass.

INTERIM TECHNICAL REPORT

ON THE DEVELOPMENT AND CONSTRUCTION OF

TWO HYDROGEN MASERS FOR THE

NATIONAL AERONAUTICS AND SPACE ADMINISTRATION
Geo. C. Marshall Space Flight Center
Huntsville, Alabama

under Contract No. NAS 8-2604

Period Covered: 1 February 1962 to 31 May 1963

FOREWORD

This report describes the work done for the National Aeronautics and Space Administration under contract number NAS 8-2604. The contract originally had as its objective the construction of two state-of-the-art atomic hydrogen masers. Work began early in 1962 and at that time the notion of an easily transportable maser was a rather tenuous one since vacuum systems to handle and dispose of hydrogen were all rather bulky, requiring diffusion pumps and the necessary cold traps. The first encouraging signs of being able to construct a compact system came from experiments then in progress with VacIon pumps which, when operated at reduced voltage, could dispose of large quantities of hydrogen, enough to give a lifetime for a hydrogen device of about one year.

While the program is one for the construction of two masers, there is the underlying necessity to develop techniques that will take the fullest advantage of the narrow resonance linewidth offered by the hydrogen maser, and the development of the maser as a frequency standard and clock is an obvious goal. There are in the hydrogen maser many inherent properties that lead to this. As already mentioned, there is the extremely narrow resonance linewidth, which can be described as having a Q of 10^9. The device is an oscillator from which power is received and thus it is different from most other atomic devices which are essentially very narrow bandwidth filters at microwave frequencies. There are two important advantages in this oscillator. The first is that it automatically seeks the center of the atomic resonance without the use of electronic or other external servo techniques. The second is that as an oscillator it provides a continuous accumulation of phase without the interruptions common to servo controlled crystal oscillators.

While it is true that the level of oscillation is low, amplification of the signal is possible with a penalty being paid in very short term phase stability (.01 sec. or less). Over longer periods, the output is characteristic of the maser and can be used to drive devices such as frequency dividers and other phase-locked oscillators providing ultra stable, phase coherent signals at any frequency in the spectrum now available to electronic devices.

As the construction phase of the contract advanced, many new ideas came to light and concepts of many problems changed. The contract was extended to include a measurement phase divided into the specific tasks listed below.

Task A -- Conduct a measurement program for long and short term stability using three hydrogen masers.

Task B -- Conduct measurements to determine the precision to which a given pair of masers can be reset with respect to frequency.

Task C -- Conduct measurements to determine very short term relative stability. Very short term is defined as 0.01 seconds or less; approximately 3 months to complete after the approval of Task B.

Task D -- Measure the ratio of cesium to hydrogen frequencies of hyperfine separation; approximately 2 months to complete after approval of Task C.

Task E -- Compare the two NASA masers with those at Harvard; approximately one month to complete after approval of Task D.

These measurements and the understanding of the effects disclosed have led to knowledge of improvements that can be made. When possible these improvements have been made and incorporated in the devices originally built for NASA. This report covers the period from the inception of the contract to the end of May 1963, and does not give the results of the various tasks in detail; however, at this time of writing much more has been learned about masers and it is desirable in this "foreword" to outline very briefly the nature of the latest advances and the direction in which future work should go.

The combination of light weight, small size, and improved stability will depend mostly on modifications to the cavity and bulb structure. A very promising advance is possible by combining these two functions in a dielectrically loaded quartz sphere about 8 inches in diameter. Mechanical and thermal properties will be improved and better thermal and magnetic shields and d.c. magnetic field control will be afforded. The size, weight, and power requirements of the present pumps can be reduced by the use of sorption techniques using outgassed titanium hydride, and systems suitable for spacecraft have become possible. For these applications it is appropriate to further revise the thinking devoted to vacuum systems. Spacecraft operate in a vacuum far more perfect than that attainable under

normal conditions on earth, and pumping systems need not be included except for ground-based testing. While the need for ultra high precision clocks aboard space vehicles may not yet have reached a crucial level, it is now possible to perform the extremely fundamental experiment of measuring the time dilatation and gravitational red shift effects to unprecedented accuracy.

Some of the work reported in this text has resulted from very constructive cooperation of the National Aeronautics and Space Administration with the United States Navy, and we are indebted to Mr. John Gregory of NASA for making this possible. The measurements of the cesium-hydrogen relationship was due to extremely close cooperation between the Office of Naval Research and NASA, and involved the following laboratories and agencies: Naval Observatory, Washington, D.C.; Naval Research Laboratory, Washington, D.C.; Bureau of Ships, Washington, D.C.; U.S. Coast Guard Loran Stations on Nantucket, Mass., and Cape Fear, N.C.; National Aeronautics and Space Administration, Astrionics Div., Huntsville, Ala.; Varian Associates Bomac Laboratories, Beverly, Mass.; and our grateful acknowledgments are extended to Mr. Myron H.C. Criswell, Bureau of Ships, Mr. John Gregory of NASA, Dr. R. G. Hall, Naval Observatory, Mr. Harris F. Hastings, NRL, Dr. William Markowitz, Naval Observatory, and Mr. R. R. Stone, NRL.

The work of developing the design and supervising the construction of these devices has been done by Mr. Harry Peters of our laboratory, and the advance of the program is largely due to these efforts. The competent and enthusiastic support of Messrs. E. R. Parsons, E. Marison, R. Cochran, R. Hamilton and W. Kilkelly have been invaluable to this work.

R. Vessot
30 January 1964

TABLE OF CONTENTS

		Page
1.0	INTRODUCTION	1
2.0	TECHNICAL REPORT	7
2.1	Frame and Vacuum Manifold	7
2.1.1	The Vacuum System	8
2.1.2	Hexapole Mounting	9
2.1.3	Source Assembly	9
2.2	Hydrogen Purifier and Flow Control	9
2.2.1	Hydrogen Pumps	10
2.2.2	Hydrogen Pumping Experiment	12
2.3	Hydrogen Discharge Dissociator	17
2.3.1	Source Collimator	19
2.4	Magnetic State Selection	21
2.4.1	The Principle of Operation of the Magnetic Hexapole State Selector	21
2.4.2	Design and Fabrication of Magnets	26
2.5	The Storage Bulb	27
2.5.1	Bulb Coating Techniques	29
2.6	The R.F. Cavity	30
2.6.1	Thermal Control	34
2.7	Magnetic Shielding and Field Controls	36
2.7.1	Magnetic Shielding	37
2.7.2	Degaussing Techniques	40
2.8	Magnetic Field Measurement	41
3.0	MEASUREMENTS AND DATA FROM HYDROGEN MASER EXPERIMENTS	43
3.1	Introduction	43
3.2	Measurements and Data	43
3.2.1	Cavity Tuning Procedure	44
3.2.2	Magnetic Field Variation	45
3.2.3	Measurements	46
3.2.4	Locking	49
3.2.5	Effects of External Noise	49

(continued)

TABLE OF CONTENTS

(continued)

		Page
4.0	WORK IN PROGRESS	51
5.0	REVIEW OF IDEAS AND INVENTIONS	54
6.0	TABLES AND PUBLICATIONS	55
	References	56
	Appendix I -- Report on the Frequency of Hydrogen, by Dr. Wm. Markowitz, U.S. Naval Observatory	
	Appendix II -- Distribution List	

LIST OF ILLUSTRATIONS

		Page Ref.
Figure 1	Section Drawing of the Atomic Hydrogen Frequency Standard	3
Figure 2	Frame Layout	7
Figure 3	Varian "Conflat" Flanges Section Drawing	8
Figure 4	Hexapole Mounting	9
Figure 5	R.F. Dissociator	9
Figure 6	Schematic Diagram of Hydrogen Handling System	10
Figure 7	Hydrogen Flow Measuring System	11
Figure 8	Re-designed Vac Ion Structure	11
Figure 9	Micro-photograph of 400 Tube Collimator	21
Figure 10	Atomic Hydrogen Hyperfine Energy Levels	22
Figure 11	Fastest and Slowest Trajectories Grazing the Magnet	24
Figure 12	The Hexapole Magnet	26
Figure 13	Cavity and Bell Jar Vacuum Envelope	32
Figure 14	Maser Upper Section Assembly Drawing	34
Figure 15	Thermal Control Circuitry	35
Figure 16	NASA Hydrogen Masers	43
Figure 17	Frequency Shift vs. Cavity Tuning	45
Figure 18	Frequency Comparison Receiver	46
Figure 19	Maser Beats	46
Figure 20	Hourly Measurements of Stability For 7 Days	46
Figure 21	Histogram of Five Days Hourly Data	46
Figure 22	Histogram of 10 Second Measurements	47
Figure 23	Hourly Measurements of Stability for 68 Days	47
Figure 24	Time Comparison System	48
Figure 25	Maser Beats vs. Crystal Oscillator	48
Figure 26	Time Measurements vs. Loran Signals	48

1.0 INTRODUCTION

The hydrogen maser is the result of a search for a new type of maser operating between two hyperfine levels in one of the hydrogen-like atoms. During the many years of research on atomic beams, the work was concentrated on atoms that were easily detected by surface ionization and had good properties for producing atomic beams. From these atomic beam experiments came a wealth of new data on the nature of the atom and, in particular, the nature of nuclear matter. The early experiments were done without the use of radio frequency energy and consisted of atomic beams passed through inhomogeneous fields; and from the deflections produced by the interaction of atomic dipole in the gradient of the field, information could be obtained concerning the spin and magnetic moment of the nucleus.[1,2]

Resonance experiments were introduced by Rabi and Kellogg in 1938.[3,4] These experiments first consisted of applying a magnetic field at the frequency of precession either of the nucleus in an external magnetic field or in the magnetic field of the electrons. Experiments on resonances at higher and higher frequencies followed closely in the wake of inventions and discoveries of high frequency r.f. sources.

It must be borne in mind that these experiments were all concerned with trajectories and the effect that r.f. transitions between levels would have on the magnetic moment of the atoms and the consequent deflection in an inhomogeneous field. The low density of the beam is desirable to weaken the interaction between the atoms, making possible "free space" measurements of very great precision. Techniques to narrow the linewidth by extending the interaction time were developed. These techniques depended on the duration of the time of flight of the atom through the r.f. interaction space and led to the invention by Ramsey[5,6] of the separated oscillatory field which later became an important feature on cesium devices used as frequency standards.

It was realized that the detection of r.f. radiation from these atomic beam devices would be very difficult because of the low densities of atoms in the r.f. magnetic fields and the difficulties of coupling over long distances with the problem of frequency shift due to Doppler effects. These difficulties were first overcome in the case of electric transitions where the interaction of the atom in the r.f. field is about 10^5 times stronger. In 1954 Gordon, Zeiger and Townes[7,8] reported the operation of an ammonia maser. This maser employed an electric state selection mechanism consisting of a multipole array of rods alternating in polarity creating a strong inhomogeneous electric field that focussed the upper state molecules into a long r.f. cavity tuned to the resonant frequency of the transition. The time of flight through the cavity is in the millisecond range and the natural line breadth is therefore large. By having a sufficiently high Q cavity and sufficiently high beam flux of state selected atoms, it was possible to operate the device as an oscillator having good stability. As refinements were made in this new technique, some troublesome properties became apparent due to the Doppler shift in the cavity and the stability of the cavity tuning which, due to the rather low line Q (or large line breadth), made the output frequency unstable. Furthermore, the complicated molecular structure led to a multi-line spectrum.

Attempts to operate a maser between magnetic hyperfine transitions continued and culminated in the invention in 1959 of the Atomic Hydrogen Maser[9,10,11] by Prof. N. F. Ramsey of Harvard University. The earlier attempts were made with cesium and other alkali metals, and various methods to extend the interaction time were tried such as buffer gases and wall coated, optically pumped cells. An important conclusion from these experiments was that there occurred a strong polarization of the atom on collision with other atoms either in a gas or as part of a wall, and that the phase of the oscillating magnetic moment was decorrelated with the r.f. magnetic field in the cavity.

In 1959 Prof. Ramsey proposed that hydrogen be tried in conjunction with a storage cell coated with a paraffine or some such substance that presented a surface of bound hydrogen atoms, and the premise that hydrogen should be far less polarizable on collision than the heavy atoms having less well bound valence electrons proved to be true. The hydrogen maser became the first device of its kind to operate between energy levels joined by magnetic dipole transitions. The success of the storage bulb method results from mechanically storing atoms using predominantly electrical forces that have very little effect on the magnetic interactions which yield the energy detected by the observer.

The atomic hydrogen maser is described schematically in Figure 1. Molecular hydrogen is dissociated by an electrical discharge and the atoms are formed into a beam and passed through an inhomogeneous magnetic field where, by virtue of the differences in the effective atomic dipole moments of the F=1, m_F = 1 and 0 states from the F=1, m_F= -1 and F = 0, m_F=0 states, the former states are focussed into the aperture of a specially coated storage bulb located inside an r.f. cavity. The atoms are confined by the bulb to a relatively uniform r.f. field having only one phase component. The cavity is tuned to the frequency of the F=1, m_F= 0 ⇝ F = 0, m_F = 0 transition. The atoms enter the bulb and, making random collisions with the wall, eventually leave through the entrance aperture. Due to the nature of the walls of the bulb there is very little interaction with the hydrogen atoms, and even though there may be as many as 10^5 collisions during one second, the atoms are not seriously perturbed.

The resonance line is therefore extremely sharp. Thermal noise processes contribute energy to the cavity which in turn stimulates further transitions, starting a self-sustaining oscillation if the energy from the atoms exceeds the losses in the r.f. fields.

As a frequency standard, the hydrogen maser has the advantage of a narrow linewidth resulting from atoms having a long interaction time in a very unperturbed condition. Doppler shifts of first order are very small

due to the average velocity of the atoms in the bulb being very nearly zero. Being a maser oscillator, the device has inherently a low noise performance, and avoids the disadvantages of electronic servos to seek the center of the line.

Research on hydrogen masers continued at Harvard and at Varian where experiments and measurements were made to investigate their properties as frequency standards and clocks. On February 1 of 1962 work began on the NASA contract, whose objective was to construct and deliver two atomic hydrogen masers according to the state of the art and to undertake studies on hydrogen pumping in order to make the device less complicated and more compact.

The state of the art was very rapidly advancing at this time and in order to take advantage of late developments the design of certain parts of the maser was left as flexible as possible, while the design of other parts, for which no outstanding developments could be foreseen, was frozen. The first parts to be designed included the mounting frame, vacuum manifold, and general pump layout, as well as the hexapole magnet assembly and its mounting hardware.

A vertical orientation was chosen. Two previous masers built at Varian had this design which diminished considerably the amount of floor space required as well as offering a more stable mounting for the r.f. cavity and shield structure.

Previous work at Varian had also pointed out the necessity of enclosing the r.f. cavity in a controlled atmosphere to avoid the detuning effects of changing humidity and barometric pressure in the interior of the cavity. The further requirement of good thermal stability made it desirable to house the cavity in vacuo to avoid the dielectric effects as well as the thermal gradients. Another advance made at Varian was the electrodeless, r.f. excited discharge tube which allowed considerable reduction in size as well as power consumption over the Wood's[12,13] tube originally used in hydrogen masers.

One of the chief uncertainties in the design of a maser for use outside the laboratory lay in the nature of the hydrogen pumps to handle the expended gas. The gas flow into the system had been reduced considerably by the use

ATOMIC HYDROGEN FREQUENCY STANDARD

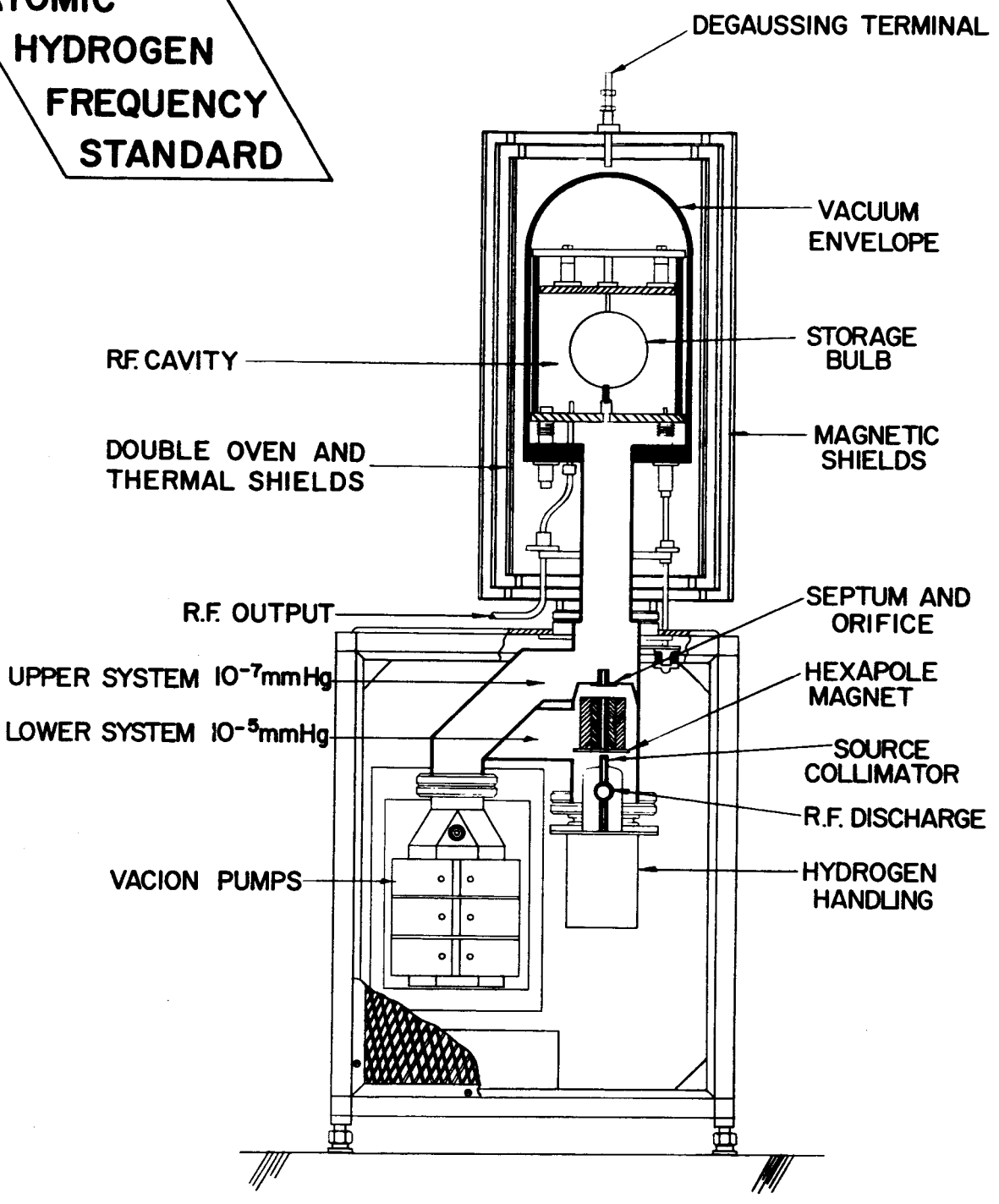

VARIAN associates
BEVERLY, MASSACHUSETTS

Figure 1

of multitube source collimators for effusing the atomic hydrogen as a well defined beam and diminishing the flux in the off-axis directions. The principal problem lay in the low vacuum scavenging pumps of the proposed differentially pumped system. This system was to be divided into two chambers in order to isolate the storage bulb from the state selection system. For a storage time of about 1 second, the total path of the average atom would be almost kilometers in distance. Molecular hydrogen does not appreciably perturb the atomic transition. (The first successful bulb linings made of paraffines and alkylchlorosilanes had bound hydrogen atoms exposed.) However, it was very desirable to limit these collisions to avoid phase decorrelations and the consequent quenching effects. The upper system was therefore isolated from the lower by means of a collimator and this system was separately pumped.

The first two masers at Varian used VacIon pumps for these upper chambers. Titanium sputtering pumps seemed extremely well suited for hydrogen as the pumping process, in principle, should proceed unaided except for maintaining clean titanium surfaces. The main question was that of total pump capacity, and a program for measuring this capacity for use in the lower vacuum system was then underway.

The manifold design was, nevertheless, frozen so that either the VacIon and diffusion pump combination or the double VacIon combination could be used. In the case of the oil diffusion pump, the trapping problem of the backstreaming oil had been solved by the use of a very large Zeolite trap. Nonetheless the system was clumsy and inefficient, and the use of two VacIon pumps seemed more promising as time progressed.

Magnetic shields for providing a low, uniform field in the bulbs were and still are a crucial necessity for operating the maser. The effect of the magnetic field* in the bulb on the output frequency is given by $f - f_o = 2750\ H_o^2$

where f is the output frequency

f_o is the hyperfine separation of hydrogen at zero field

H_o is in oersteds.

---

* Actually, the average of the square of the magnetic field over the volume of the bulb.

Apart from causing this shift in frequency, the magnetic field through its gradients can cause spurious transitions among the magnetic substates, thus quenching the oscillating moments of the atoms. The magnetic field dependence also causes atoms that have different trajectories in the inhomogeneous field to have different total phase angles, thus smearing out the net magnetic oscillating vector and, in effect, quenching it. A later part of this report will deal with these processes. The importance of the shields is great and considerable care has been exercised in the design, fabrication, and procurement of metals for them.

In reporting this work, the design and development of the various components will be described. Detailed drawings will be used where necessary; schematic drawings will be used to illustrate ideas.

2.0 TECHNICAL REPORT

2.1 Frame and Vacuum Manifold

From the experience gained in the research of other masers, it was concluded that the vertical orientation of the maser was better suited to mechanical stability of the cavity and bell jar assembly. Several factors entered into this decision. Since the cylindrical cavity to be used was built of several pieces, the best orientation for mechanical stability was to have the axis vertical and avoid cantilevered structures that might flex or, in time, deform under gravity. The support for the bulb inside the cavity also could more easily and better be made in this orientation. Consideration of thermal stability of the bell jar assembly demands that the connection to the pumping manifold offer as little thermal conduction as possible. The vertical orientation requires a less strong supporting structure and consequently less heavy wall thickness for the connection to the manifold than would be required for a horizontal layout.

The further considerations of compactness also favor the vertical design although these are not, at present, of primary importance.

It was then decided that, if possible, the maser should be self-contained and should only require to be connected to the power mains and their outputs to a suitable receiver system. As time progressed and the confidence in the VacIon pumps increased, it was decided that it was impossible to build a self-contained unit and the frame layout was made to include the VacIon power supplies as well as the thermal and field control electronics, the r.f. discharge electronics and the gas handling system. The frame layout is shown in Figure 2. The details of the end view can be related now to Figure 1 showing the manifold layout.

As will be seen in the discussion of the vacuum manifold, the apparatus is heavy and there is needed a very strong support at the flange joining the lower system to the bell jar magnetic and shield assembly.

To reduce the amount of magnetic material in the vicinity of the maser, the frame was made of aluminum extruded into a box section equipped with a ledge intended for the mounting of side panels. A plate of aluminum $\frac{3}{8}$" thick is fastened to the top of the frame and supports the maser vacuum system assembly at the junction of the upper and lower systems.

2.1.1 The Vacuum System

The vacuum manifold is designed to allow dismantling and changes within the bell jar as well as the lower system where are located the source, hexapole and the pumps. Two systems connected by a collimated orifice form the vacuum manifold. The lower system, enclosing the source and state selector, is pumped by a specially modified 75 ℓ/sec VacIon pump operated at low voltage. This part of the system is operated at about 10^{-6} mm. Hg pressure and is isolated from the upper system where a pressure of better than 10^{-7} mm. Hg is maintained.

The entire manifold outside the upper magnetic shields is fabricated of type 304 stainless steel tubing. The vertical section enclosing the hexapole is made of 6" diameter 0.040" wall and has welded within it a septum made of inconel to which is fastened the collimated channel connecting the upper and lower chambers. The inconel septum also serves as a magnetic shield for the hexapole. Tubes from these two chambers lead each to a VacIon pump. Both pumps are located within a common magnetic shield assembly. The polarities of the magnets are arranged so as to form a quadrupole in order to reduce the shielding problem.

Flanges of the Varian Con-flat type are used for vacuum-tight joints throughout the system with the exception of the bell jar seal. These flanges employ a copper gasket into which a sharp edge is forced by tightening the joint. Radial expansion of the gasket is prevented by a recess in each flange. Figure 3 shows a typical flange of this type. In all, four sets of flanges are used and allow the system to be taken apart at the pumps, the source and the upper bell jar assembly.

Figure 2

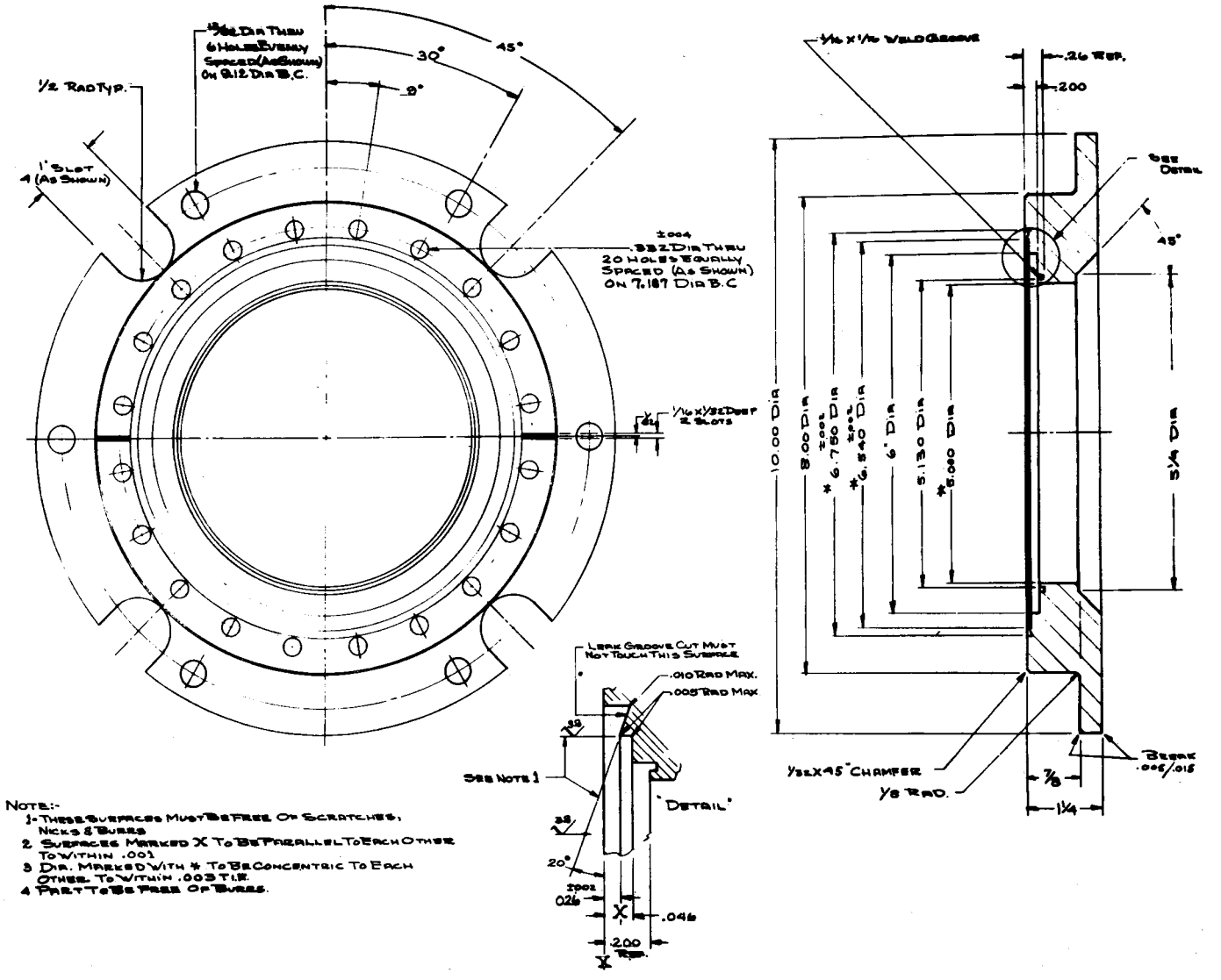

NOTE:-
1- THESE SURFACES MUST BE FREE OF SCRATCHES, NICKS & BURRS
2 SURFACES MARKED X TO BE PARALLEL TO EACH OTHER TO WITHIN .001
3 DIA. MARKED WITH * TO BE CONCENTRIC TO EACH OTHER TO WITHIN .003 T.I.R.
4 PART TO BE FREE OF BURRS.

Figure 3

2.1.2 Hexapole Mounting

The hexapole magnet is mounted in the manifold and fixed to it by the following scheme.

The magnet is fastened to three posts each reaching down to a ring recessed into the lower VacIon flange. This assembly, shown in Figure 4 provides the vertical positioning of the magnet. Three radial screws from the magnet mounting ring bear on the walls of the manifold to provide lateral adjustment and positioning. The magnet is visually aligned with the axis of the manifold and bell jar - cavity assembly. After this is done the septum is adjusted and tightened into position.

2.1.3 Source Assembly

Since the state selecting magnet and the storage bulb are fixed, it was thought advisable that the source of hydrogen atoms be adjustable in position. Figure 5 shows the flexible bellows assembly used to mount the source. One end of the 4" stainless steel bellows is copper brazed to a Con-flat flange mating to the manifold; the other end is brazed to a stainless steel flange to which is welded the Kovar sleeve onto which is sealed the glass r.f. discharge tube. Three screws threaded into the lower flange and bearing against the conflat flange provide the adjustment of the source position in the magnet. The lower flange also provides a location for the glass parts of the gas handling system which moves together with the source. Connection of the gas handling system with the hydrogen supply mounted to the frame is made by a flexible small diameter copper tube.

2.2 Hydrogen Purifier and Flow Control

The design of this part of the apparatus followed closely that which had been found to be successful in the experimental masers previously built*. In these systems the glass discharge tube was connected directly to a palladium

---

* Contract Nonr 3570(00)

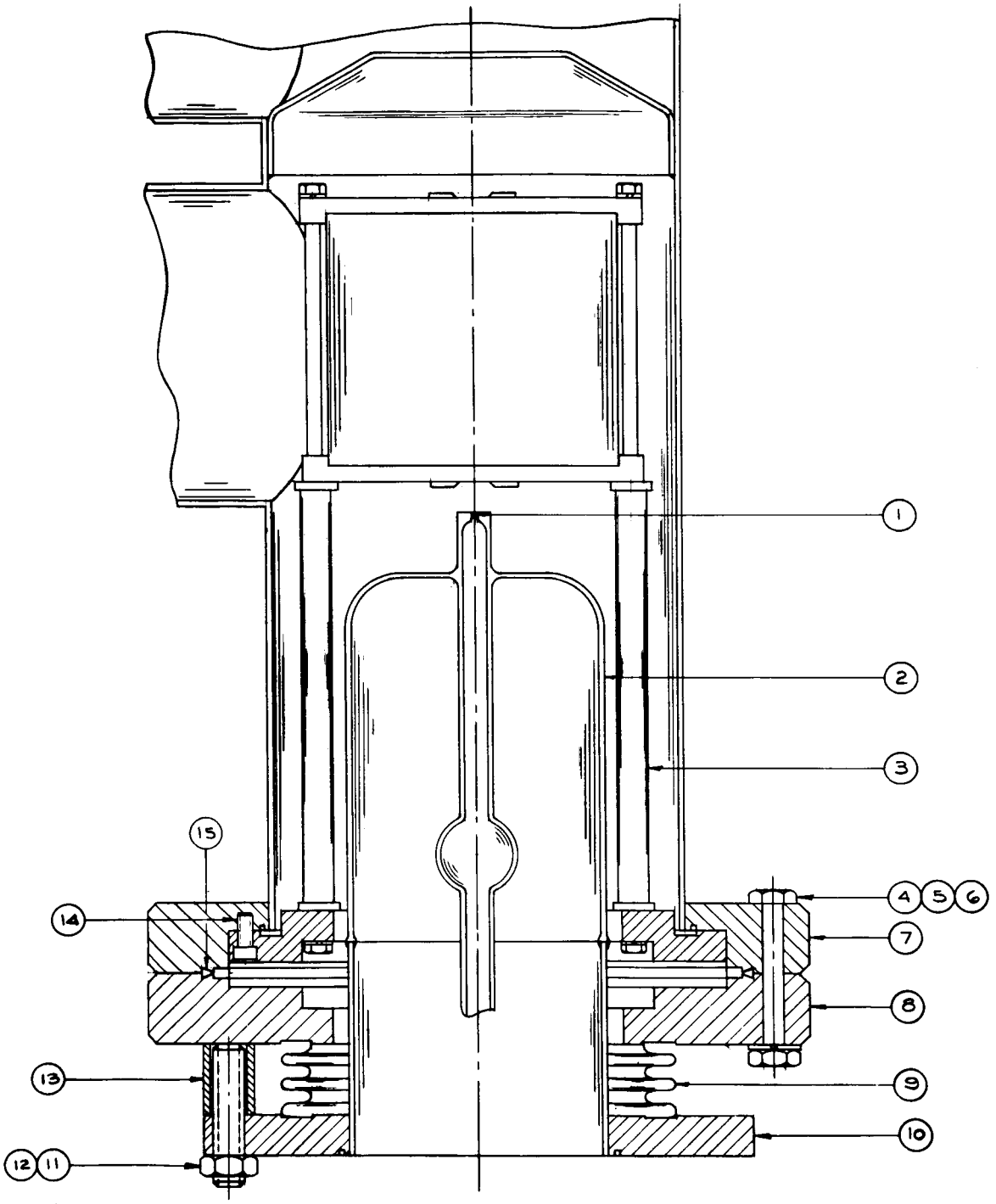

Figure 4

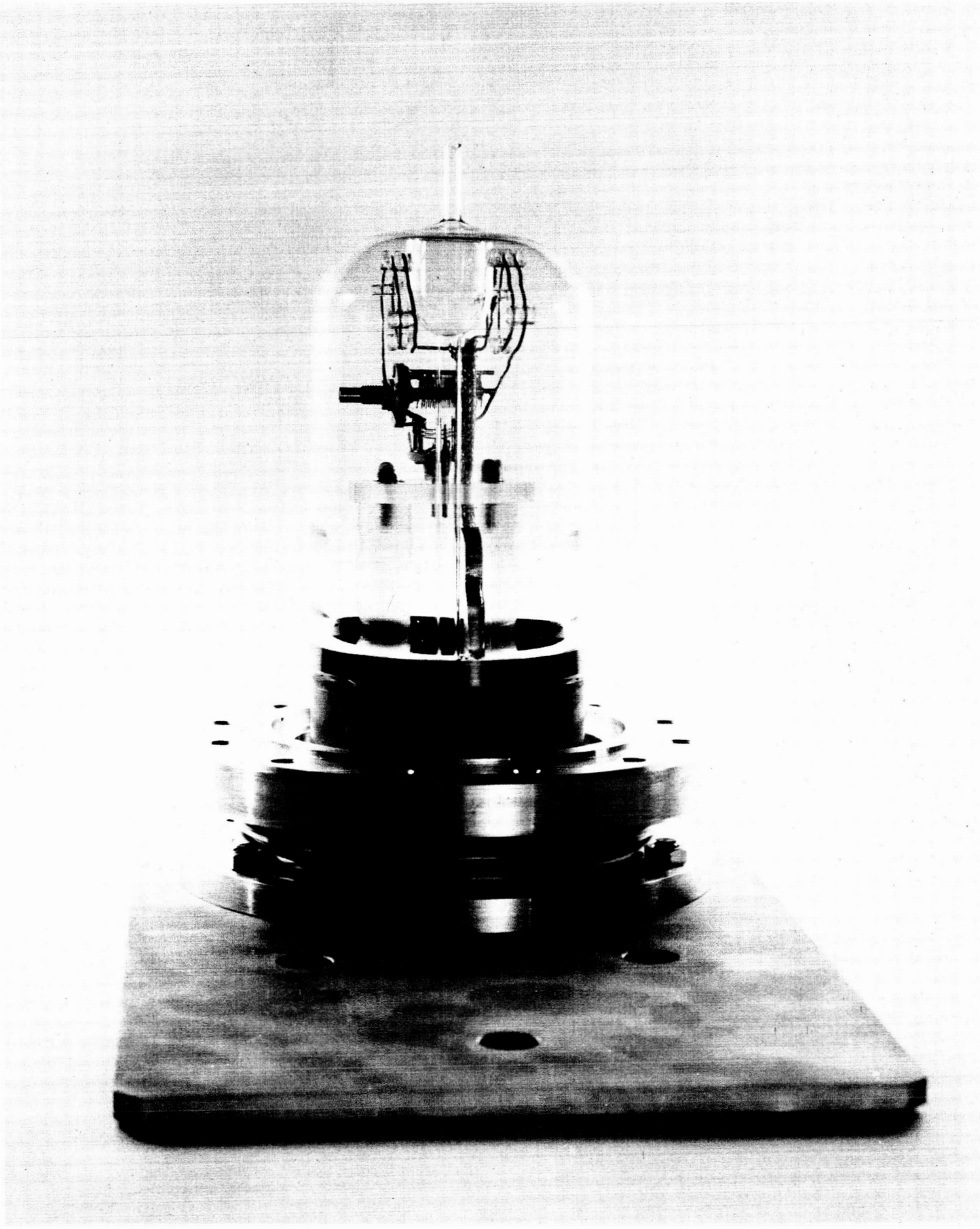

Figure 5

tube purifier which, in turn, was fed from a VEECO* variable leak. The control of the flow rate depends on the setting of the variable leak which is fed from a pressure regulated supply of hydrogen. Hydrogen pressure at the source and at the impure side of the purifier is measured by Pirani gauge tubes that connect to the measuring instrument, in this case a CVC+ Autovac gauge. The system is shown schematically in Figure 6.

Coarse adjustment of the flow is provided by the variable leak; however, experience has shown that this device cannot be used for any reproducible setting of flow. The fine adjustment is made by varying the pressure from the regulator and, normally, a pressure from 2 to 3 lbs. per square inch is necessary. The palladium tube offers another means of flow control and this is used for tuning the masers, and will be described later.

Flux measurements can be made by the following method. Since the volume of the glass bulb surrounding the palladium thimble is known and the pressure of the enclosed gas can be monitored, the rate of flow of the atoms can be obtained from the relation

$$PV = n\,RT$$

$$V\frac{dP}{dT} = \frac{dn}{dt}\,RT$$

$$= Q$$

The relation between the pressure and the flow at that pressure can be determined. Since the measurement is made over a long period of time (approximately 10 minutes), the static relationship between flow and pressure is not far different from that obtained by this dynamic method. From these data the threshold level of oscillation and other quantities such as pump capacity can be measured.

2.2.1 Hydrogen Pumps

The decision to use VacIon pumps came as a result of the successful operation of a pump over a period of 218 days at a greater rate of flow than

---

* Vacuum Electronics Corp., Long Island, N.Y.

\+ Consolidated Vacuum Corp., Rochester, N.Y.

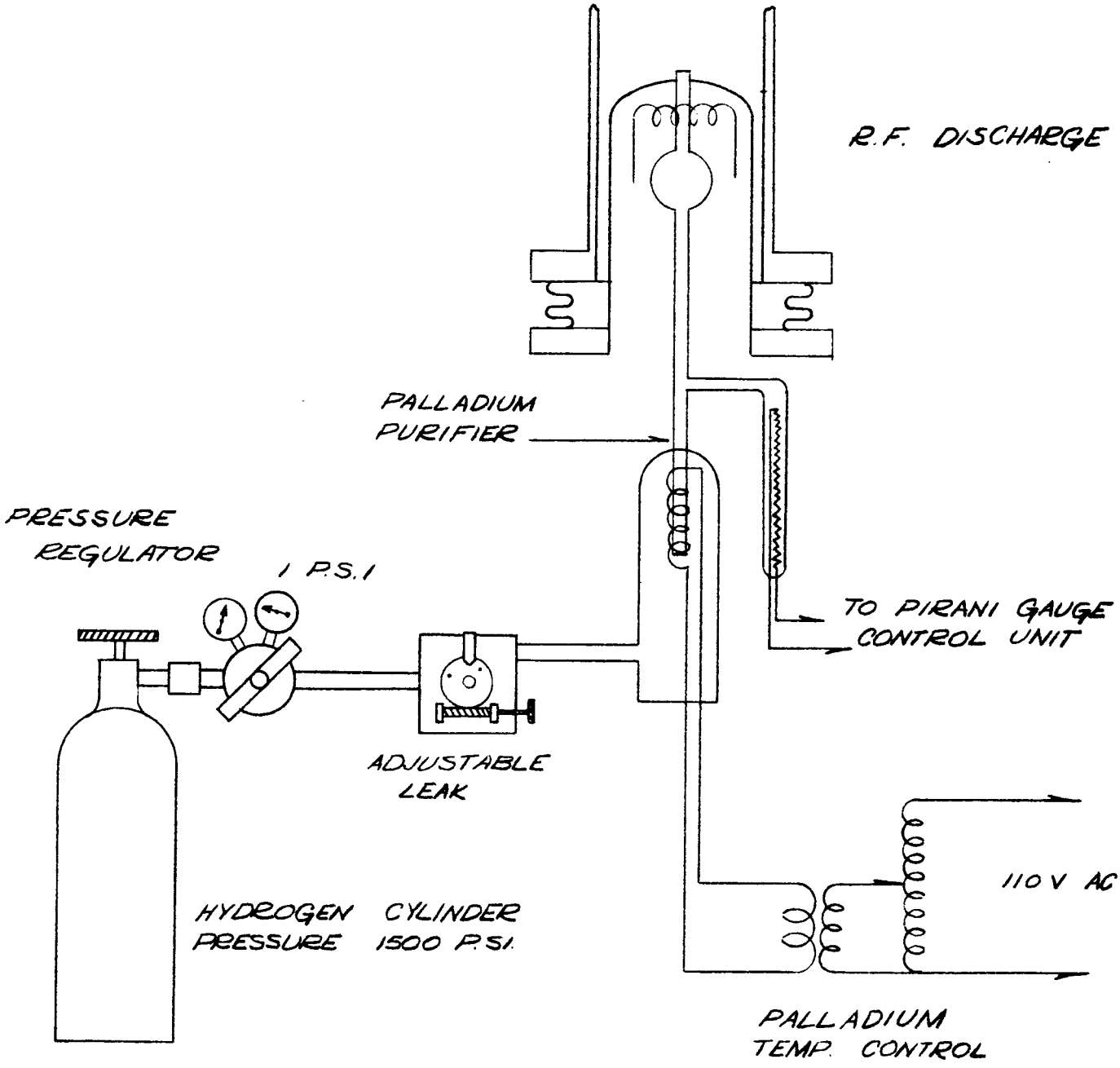

DIAGRAM OF HYDROGEN HANDLING SYSTEM

FIG. 6

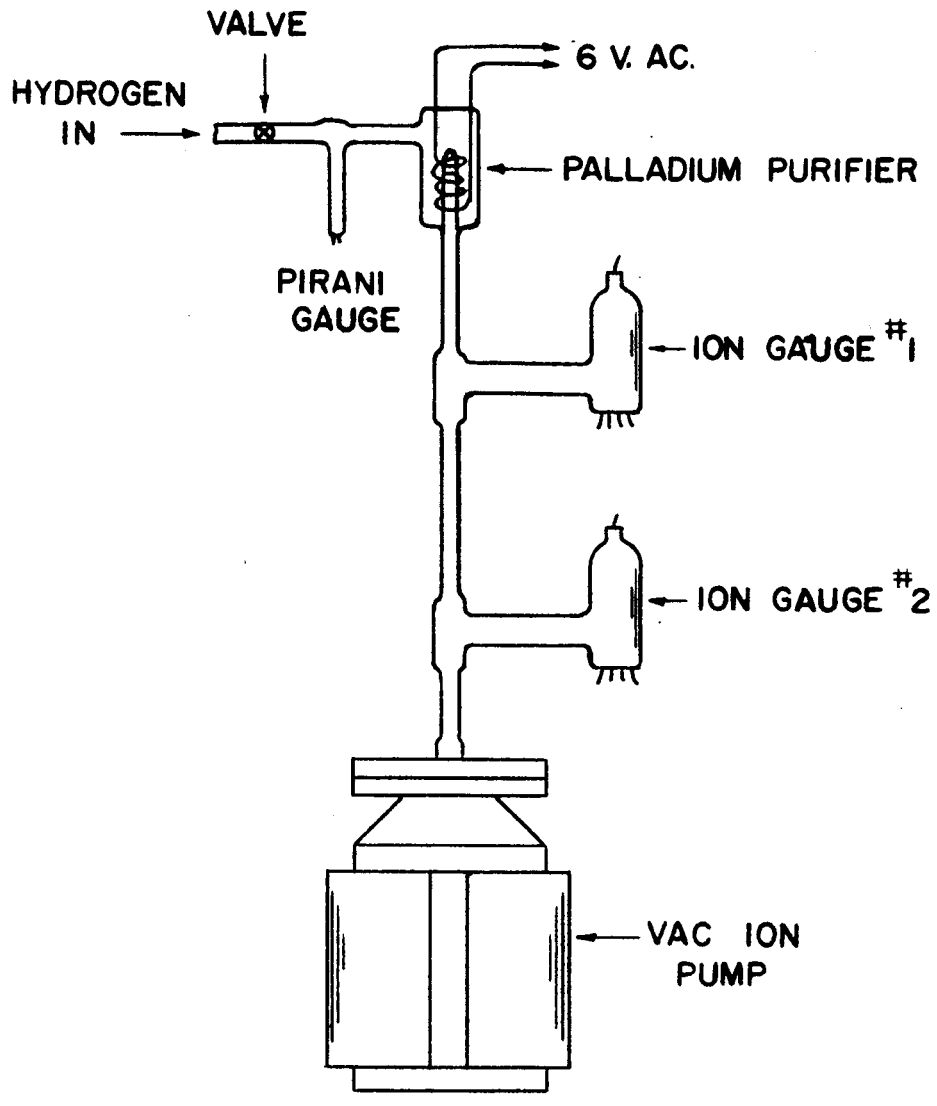

HYDROGEN FLOW MEASURING SYSTEM

FIGURE 7

that needed to operate a maser. The experimental system is shown in Figure 7, and the data are given in the following section.

It was found that the pump would operate at reduced voltage, thus diminishing the amount of heat dissipated by the cathodes. In time, as the pump collected more and more hydrogen, it became important not to heat the cathodes since this caused them to release hydrogen. The discharge was maintained at 1.5 Kv. and 1.5 ma. and served only to keep the titanium surfaces clean so that they could assimilate the hydrogen. The pump ran for 202.25 days, at the end of which the cathode and anode short circuited. On dismantling the pump, both the anode and the cathodes were found to be severely distorted. This was expected for the cathodes but not for the anode. The anode electrode, also made of titanium, was not subject to positive ion sputtering, but nevertheless, since the system was so clean, became well enough scrubbed by electrons and negative ions that it also contributed to the pumping. Since the area of the anode structure is large and the cells made of thin metal, the structure warped seriously when it combined with an appreciable amount of hydrogen. The cathodes, made of slabs of $\frac{1}{8}$" titanium, are supported at their ends and tend to warp inwards toward the anode as the titanium combines with hydrogen. This was the reason for pump failure. The titanium was far from saturated and needed to be properly supported to continue operation. A redesigned structure was built and is now operating (as shown in Figure 8).

This new structure consists of titanium cathodes that are supported both at the ends and at the middle and incorporate slots to relieve the stress and prevent warping over large distances. The anode structure has been made of stainless steel and will no longer combine with hydrogen, and therefore should remain intact.

Further data on pumping by a VacIon device is being obtained from the operation of such pumps on the two masers.

2.2.2 Hydrogen Pumping Experiment*

A VacIon pump was set up to determine its ultimate capacity. The system is as shown schematically in Figure 7 and consists of a palladium purifier leading to a flow measuring system connected to the VacIon pump. Two methods of measuring the flow are employed. The first uses the known volume and rate of change of pressure of the gas in the bulb of the purifier as measured by a Pirani gauge that was previously calibrated by using a McLeod gauge. The second method is by measuring the pressure drop across a constriction of known speed. A further but not very accurate method uses the VacIon current as a measure of the pressure in the pump. This last method is not directly related to the rate of the pumping in that direct chemical combination of atoms with the titanium is not accounted for. The data from this experiment are given in Table 1 and the calculations of the flow measuring system and measurement of the gauge constants are given below.

Table 1

Period	Operating Days	Flow Rate Atoms/Sec.	Quantity Pumped Moles of H_2
11 Dec. 1961 to 27 Dec. 1961	16	1.25×10^{17}	.14
27 Dec. 1961 to 19 July 1962	202.25	7.56×10^{16}	1.10
Total moles of gas pumped =			1.24

Calibration of Flow Measuring Equipment

The pumping speed of the tubulation between the ion gauges is obtained as follows:

Length of tube = 29.0 cm. = ℓ

Inside diameter = 1.05 cm.

Radius = $\frac{1.05}{2}$ = .525 cm. = α

* This work was supported by the Office of Naval Research under contract Nonr 3570(00).

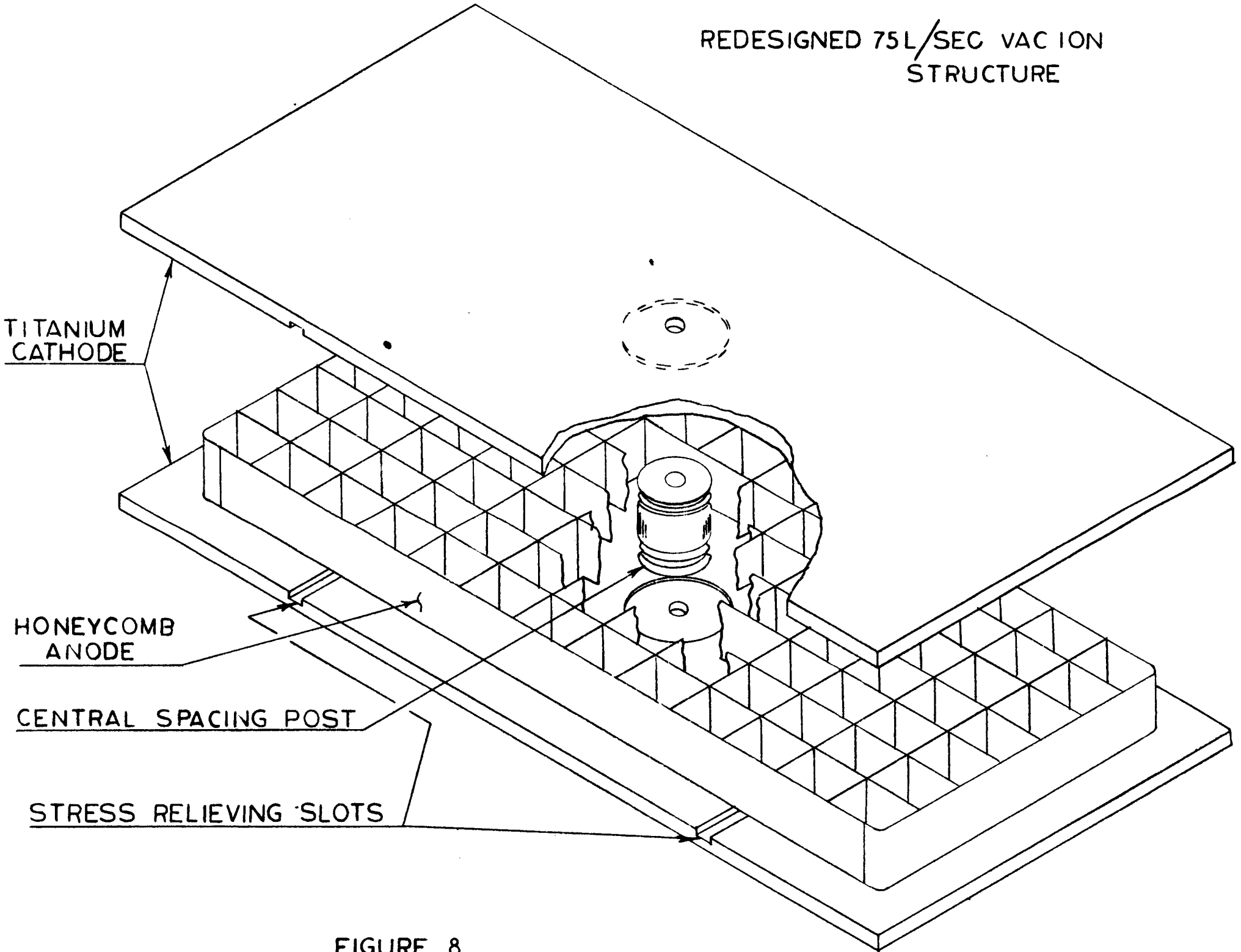
REDESIGNED 75 L/SEC VAC ION
STRUCTURE
TITANIUM
CATHODE
HONEYCOMB
ANODE
CENTRAL SPACING POST
STRESS RELIEVING SLOTS

FIGURE 8

Referring to Dushman,* Chapter 2, p. 101,

$F = KF_o$ = speed of tube

$F_o = 11.428\,\alpha^2\sqrt{\frac{T}{M}}$ = speed of orifice at absolute temperature T for a gas of molecular weight M

with $T = 298^0K$, for hydrogen,

$F_o = 32.25$ liter/sec.

From Table 3, p.99,

with $\ell/\alpha = 29.0/.525 = 55.2$

$K = .0458$

and $F = (.0458)\ (38.25) = 1.75\ \ell$/sec.

The ion gauge constants may be obtained from dp/dt measurements as follows:

V = Volume of palladium purifier high pressure side and attached tubulations, pressure gauges, traps, valves, etc.

Assuming the pressure, P, is uniform in this volume, the rate of evolution through the purifier when the hydrogen supply value is closed may be found. Let $M = PV$ = total quantity of gas in V at any time, t. Then the evolution rate, Q, is given by

$$Q = -\frac{dM}{dt},$$

so $Q = V\ (-\frac{dp}{dt})$ since V is constant.

Let P_V = pressure at upper ion gauge and P_L = pressure at the ion gauge.

Then $Q = F\ (P_V - P_L) = F\ P_V\ B$ (1)

where $B = (1 - \frac{P_L}{P_V})$ and F is the pumping speed.

---

* Vacuum Technique, Saul Dushman, John Wiley & Sons, Inc. (1958).

The ion gauge calibration factor, K, is given by*

$$K = \frac{I_c}{I_g P}$$

where I_c is the collector current, and I_g the grid current.

Inserting the value of P from (1),

$$K = \frac{I_c F B}{I_g Q} \quad . \tag{2}$$

The values of K found may be compared with published values for similar ion gauge structures.

The dp/dt measurements also give the flow rate directly. By taking ion gauge readings at the same time, the rates may be independently measured at pressures corresponding to constant operating conditions.

Two types of ion gauges were used in these experiments. The first experiment used gauges with structures made of tantalum and were of a geometry similar to commercially available gauges having gauge constants of about 25 for nitrogen. The hot tantalum metal, however, absorbs and becomes embrittled by hydrogen, so new ion gauges have been obtained which have tungsten structures. These gauges are geometrically similar to older ion gauges which have gauge constants of about 12 for nitrogen.**

As given by Alpert, the gauge constant for hydrogen is approximately .5 that for nitrogen.

The second hydrogen pumping experiment described in the text was set up with one gauge of each type at the upper end of the tube construction, so that calibration factors could be obtained between the two types at the same pressures. The ratio of their gauge constants was found to be $1.45 \pm .01$. Thus the gauge readings are related by I_c (tantalum structure) = $1.45\ I_c$ (tungster structure).

---

* "Production and Measurement of Ultrahigh Vacuum," D. Alpert, Handbuch der Physik 13, Springer-Verlag (Berlin, 1957).

Before giving the calibration factors obtained by the dp/dt measurements, it must be borne in mind that there are very important sources of error in using this technique. The largest errors appear to be due to the evolution of gas from the walls, or in flux from other sources such as leaks or virtual leaks, etc., within the volume, V. Another error can be due to variation in the quantity of hydrogen contained within the palladium metal of the purifier during the course of measurements. Non-uniformity of pressure and pumping of the ion gauges are other possible sources. In addition, variations of 20% or so between similar gauges from different manufacturers are possible.

First measurements were performed using a McLeod gauge. Flow rates and gauge constants are given below.

Pressure - mm. Hg	Flow Rate - mm. -ℓ/sec.	K
1.5	1.22×10^{-3}	8.01
1.0	7.3×10^{-4}	7.61
.5	3.51×10^{-4}	6.67

These rates are likely to be low, as are the values for K, since the volume involved has sources of influx of gas. This was evident from pressure rises in the sealed off system.

A Pirani gauge installed near the palladium purifier would give data less subject to the above errors. The rest of the data for pumping experiment No. 1 was obtained this way. Typical results are given below.

Date	Pirani Pressure, mm. Hg	Rate mm. -ℓ/sec.	K
12-11-61	2.70	1.29×10^{-3}	9.5
2-8-62	1.80	1.24×10^{-3}	9.5
2-11-62	3.50	1.50×10^{-3}	10.2
2-15-62	2.80	1.27×10^{-3}	9.77
4-17-62	3.25	1.83×10^{-3}	11.8
4-17-62	1.75	1.23×10^{-3}	10.54
5-17-62	3.10	1.57×10^{-3}	12.3
5-17-62	1.80	1.03×10^{-3}	12.2

From these data, and in consideration of published values, assumption of a gauge constant for hydrogen of 10.0 for ion gauges with tantalum structures and of 7.0 for those with special tungsten structures should involve errors of no more than ± 15%. Further experimental work should reduce this uncertainty greatly.

The second hydrogen pumping experiment incorporates the new VacIon pump cathode structure described in the text. The data is given below.

Table 2

Period	Operating Days	Flow Rate Atoms/sec Hydrogen	Quantity Pumped Moles (H_2)
31 Jan. '63 to 11 Feb. '63	11	4.64×10^{16}	.037
11 Feb. '63 to 18 Apr. '63	67	7.02×10^{16}	.247
Total Quantity Pumped to Date =			.284 moles H_2

There is no obvious reason why this pump should not operate much longer than the unmodified VacIon pump in the first pumping experiment. The theoretical maximum is 1.75 atoms H_2 for each one of titanium. The mass of the pump cathodes is measured as 660 grams, which is 13.8 moles of titanium. So, if only one atom of H_2 for each atom of titanium proves to be a practical maximum concentration, there would be a capacity of 6.9 moles of hydrogen atoms for one pump, or 3.45 moles of H_2.

Since the present pumping rate is approximately 1.35 moles per year, the total operating lifetime for a pump may be on the order of three years. This is at the rate of flow used in the second hydrogen pumping experiment, which is a rate somewhat higher than that needed to scavenge the beam in a hydrogen maser.

2.3 Hydrogen Discharge Dissociator

The first hydrogen masers were operated using a Wood's discharge tube to dissociate the molecular hydrogen. This form of discharge tube uses a long column of gas between two electrodes that apply a d.c. field to the gas. High voltages are needed resulting in considerable heating and sputtering at the cathode. As first used by Wood,[12,13] the gas admitted contained water vapor that acted as a buffer to prevent recombination. Later versions, used on hydrogen masers, used a wall coating of dimethyldichlorosilane (drifilm) to prevent recombination, as the presence of oxygen with its strong magnetic properties was undesirable. These properties cause magnetic relaxation in the bulb and consequently affect the operation of the maser.

The size, power consumption and general unwieldiness of the Wood's tube resulted in the development of a radio frequency discharge dissociator for the maser. This technique is not new and has been described in the work of Nagle, Julian and Zacharias,[14] as well as that of Davis, Feld, Zabel and Zacharias.[15] Some guidance in the design of these discharges can be obtained from the book by Sanford Brown[16] where the relationships between the pressure, frequency of the applied field, and the size of the confining vessel are explained. The design of the discharge begins with the flux needed to enter the focussing magnet as well as the cross-section allowable at the source in view of the size of the aperture of the focussing magnet. For a given flux the two parameters, aperture and flux, determine the pressure in the dissociator. Consideration of beam collimating to reduce the flux in unwanted directions will follow later. The source pressure normally is in the range

0.01 to 0.1 mm. Hg with apertures of about 0.5 to 0.8 mm., and for frequencies near 100 mc. the discharge vessel is about 3. cm. in diameter. Under these conditions easy starting of the discharge is assured.

The interaction of r.f. fields with the gas can occur both in the electric and magnetic mode. R.F. magnetic fields will cause a toroidal motion of electrons in the discharge and the coupling can be described by

$$\nabla \times E = -\frac{\partial B}{\partial t}.$$

This method has the advantage that there is less bombardment of the walls of the vessel by charged particles and consequently less erosion of the wall coatings.

Electric excitation of the discharge offers the best means of coupling the energy to the gas. The electrode structure is simple and the resonant coupling circuit should be designed with a high L/C ratio to obtain high electric fields. Provision should be made for tuning the discharge resonator as the electric characteristics of the discharge region will change considerably when the discharge is started and the circuit requires retuning once the discharge is lit.

Erosion of the wall coatings has been found to occur and, fortunately, with electric excitation the glass itself has been found to provide a relatively non-relaxing surface. The problem of erosion of the surface still exists and a noticeable decomposition of the glass has been found to occur with the products of this erosion and decomposition deposited as a dark film near to, but not at the position of the electrodes. Analysis has shown that these products contain no carbon. The films conduct electricity only slightly and seem to consist of Boron Silicon compounds, possibly B_3Si or B_6Si from decomposition of the Borosilicate glass of which the source vessel is made.

Problems with the discharge have sometimes occurred when the power level is raised to a high level or when the electrode position has been changed. At these times the discharge changes in color from the bright red associated with atomic hydrogen to a pale lavender color and even a brownish white color. This condition is not permanent and after a few more hours of

operation the red color of atomic hydrogen returns. A spectroscopic analysis of the discharge under these anomalous conditions is planned and further source experiments are also planned with substances that might be used to line the source. The requirements are that the source lining must not recombine hydrogen and also must not decompose in the discharge.

Substances such as quartz glass, Vycor, etc., do recombine hydrogen.[17] It is possible that Boron Nitride (either in polycrystalline or epitaxial form), Alumina, and some stable Titanium compounds might provide a solution. Methods of exciting the discharge in a less destructive way may also provide a solution.

The glass sources, however, continue to operate well when left undisturbed and some have been in steady operation for over a year with good results.

The r.f. power for the discharge is obtained from a very simple vacuum tube device consisting of an oscillator, tripler and power amplifier. The output frequency is about 112 mc/sec. and the power level is about 10 watts. The r.f. circuits and the coupling configuration for the discharge are shown in Figure 5 .

2.3.1 Source Collimator

The purpose of the source collimator is to reduce the flux of atoms in the off-axis directions. Ideally, the solid angle of the beam from the collimator should match the entrance solid angle of the hexapole. The magnitude of the source pressure determined, firstly, by the flux requirements and, secondly, by the r.f. discharge conditions, also determines the design of the collimator. A necessary condition for collimation by a long narrow channel is that the mean free path in the source be longer than the length of the channel. Otherwise, collisions will occur in the channel and off-axis scattering will result. In a following section it will be shown that the source pressures will be between 2×10^{-1} and 2×10^{-2} mm. Hg.

This large range of pressure is necessary for implementing the cavity tuning technique which employs spin exchange collisions as a means for quenching the oscillation and hence, varying the effect of detuning of the maser cavity.

The highest practical pressure in view of the pumping speed available is about 0.2 mm. and at this pressure the mean free path, λ, given by

$$\lambda = \frac{1}{3\pi\eta\delta^2} \qquad \eta \text{ is density of atoms}$$

$$= 1.7 \text{ mm.} \qquad \pi\delta^2 \text{ is the collision cross-section} \doteqdot 6.4 \times 10^{-16} \text{ for atomic hydrogen.}$$

For the length of the collimator always to be less than this mean free path, a value of 1 mm. has been chosen. Given the length of the collimator, the diameter, d, of the tubes is chosen so as to give a collimation angle, ℓ/d, matching the entrance half-angle of the magnet. The maximum entrance half-angle of the magnet is 3.4×10^{-2} radians.

The diameter of the collimator tube is given by

$$d = \theta\ell$$
$$= 3.4 \times 10^{-2} \text{ mm.}$$

Ideally, then, the collimator should consist of a cylindrical aggregate of these tubes each of infinitesimal wall thickness and the whole to have an over-all diameter of 1 mm.

In practice, the collimator is made of 400 tubes each having a diameter of 0.038 mm. with walls 0.005 mm. thick. These are fused together by the following method. Hundreds of small tubes having approximately 3 times the dimensions noted above are drawn from larger pyrex (Corning 7740) glass tubes. These are cut into lengths of 5 cm. and sized into batches of about 400 tubes each. A sleeve about 1.2 mm. o.d. with a wall of about .07 mm. is drawn from a larger piece of Nonex glass (Corning 7720). This sleeve is filled with the smaller tubes, taking care that all lie in the axial direction of the sleeve. The ends of the loaded tube are each fused together and to a

piece of glass cane. The aggregate is placed in a controlled oven and carefully softened and stretched about 3 times its length and allowed to cool. In cooling, the outer skin cools faster but hardens at a lower temperature than the inner tubes, allowing the whole to harden at nearly the same rate. The outer glass sleeve has 3×10^{-7} cm/cm/^{0}C more rapid thermal expansion than the inner tubes and in cooling, compresses the tubes together. The tubes, fused to each other and to the outer skin, are cut into the desired lengths using a diamond wheel and later cleaned in an ultrasonic bath. Each is inspected, photographed and graded accordingly. Figure 9 shows a microphotograph of a 400-tube collimator made in this way.

2.4 Magnetic State Selection

Multipole focussing devices have been studied by Bennewitz and Paul,[18] Friedburg and Paul,[19,20] as well as by Christensen and Hamilton[21] and Lemonick, Pipkin and Hamilton.[22] Since the time of these references, a great deal of use has been made of these devices for focussing beams of atoms and molecules.

A very brief description of the focussing action will be given. This will be followed by the calculation of beam intensities using the extreme trajectories method.

2.4.1 The Principle of Operation of the Magnetic Hexapole State Selector

The energy, W, of an atom having a magnetic dipole moment, μ, in an externally applied magnetic field, H_o, is $-\mu H_o$. Now if μ is constant in magnitude and parallel to an associated angular momentum, and if changes in H are slow compared to many periods of Larmor frequency $\omega_L = \frac{\mu H_o}{I\hbar}$, * then the projection of μ on H_o is constant and the potential energy, W, is proportional to $\mu \mid H_o \mid$.

The force on an atom is given by

$$F = -\nabla W = -\frac{\partial W}{\partial H_o} \nabla H_o.$$

---

* $I\hbar$ is the angular momentum of the atom.

When the moment is independent of H_o, the energy W is written

$$W = -\vec{\mu} \cdot \vec{H}_o = -\mu_{eff} H_o$$

then $$F = -\frac{\partial W}{\partial H_o} \nabla H_o = \mu_{eff} \nabla H_o .$$

In general, there is some dependence of the moment on H_o and the term $-\frac{\partial W}{\partial H_o}$ is referred to as the effective component of the magnetic moment in the direction of ∇H_o.

Figure 10 shows the behavior of the hyperfine energy separation of atomic hydrogen with magnetic field. The quantum number F results from the coupling of the magnetic moment of the electron with that of the nucleus and is numerically equal to the total angular momentum of the coupled system (in units of h). The coupled system can exist in two states, $F = 1$ and $F = 0$, and the three degenerate components of the upper state, $F = 1$, can be resolved by a small magnetic field. As the field is increased, the coupled energy of the particles becomes small compared to their energy in the applied field, and eventually the coupling energy becomes negligible compared to the energy of the particle in the field (Paschen-back region). The energy of this interaction in the intermediate region can be described exactly by the Breit-Rabi formula[23]

$$W(F,m) = -\frac{\Delta W_o}{2(2I+1)} - \frac{\mu_I}{I} H_o m \pm \frac{\Delta W_o}{2}\left[1 + \frac{4m}{2I+1}x + x^2\right]^{\frac{1}{2}}$$

where $$x = \frac{\left[-\frac{\mu_J}{J} + \frac{\mu_I}{I}\right] H_o}{\Delta W_o}$$

$$= \frac{(g_I - g_J)\,\mu_o H_o}{\Delta W_o}$$

$$\doteq -\frac{g_J \mu_o H_o}{\Delta W_o} \quad \text{since } \mu_I \ll \mu_J$$

μ_o is the Bohr magneton,
the plus sign is taken for the upper state and minus for the lower,
I is the angular momentum of the nucleus in terms of $\hbar$,
ΔW_o is the energy separation at zero field.

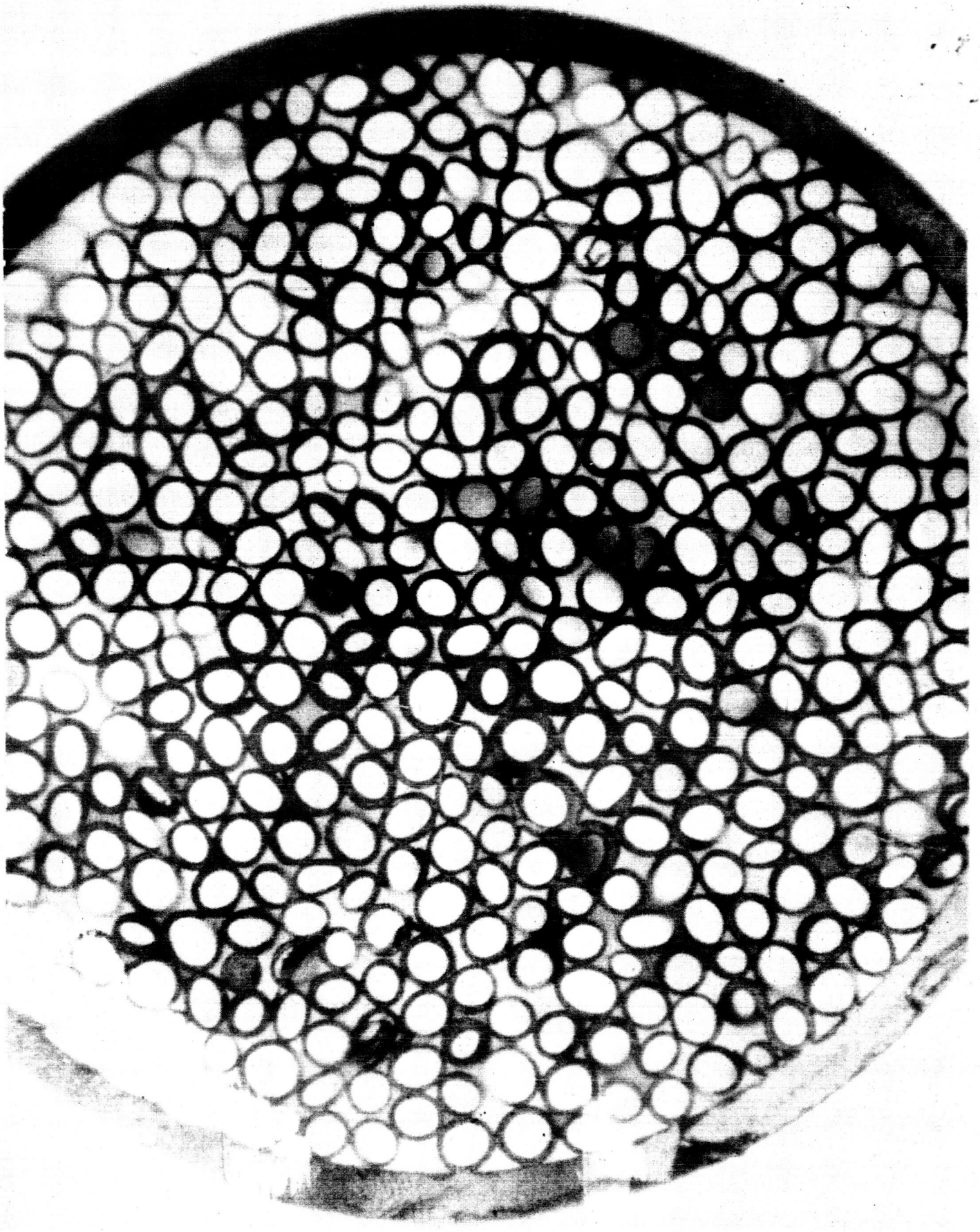

Figure 9

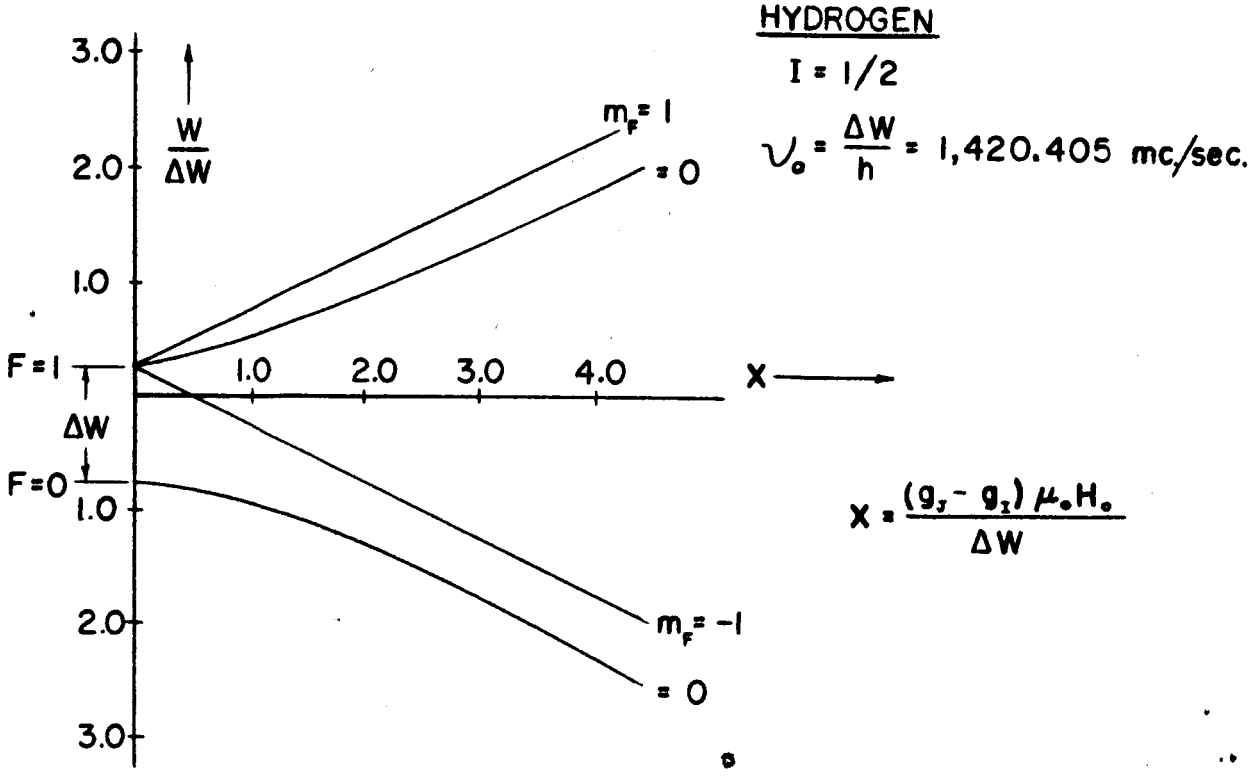

ATOMIC HYDROGEN HYPERFINE ENERGY LEVELS

FIGURE 10

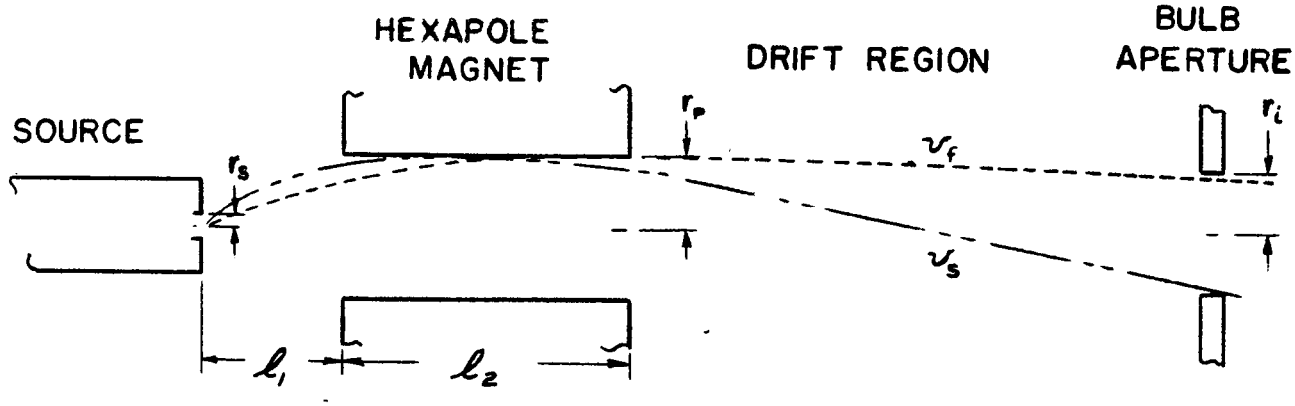

FASTEST AND SLOWEST TRAJECTORIES GRAZING THE MAGNET

FIGURE 11

The hexapole field is one of a family of multipole fields characterized by a magnetic potential function sin n θ, where θ is the azimuthal field coordinate. The field $|H|$ is proportional to r^{n-1}. In the case of the hexapole, $n=3$ and $|H|$ is proportional to r^2. This is usually written as

$$H_o = H_p \left[\frac{r}{r_p}\right]^2$$

where H_p is the field at the pole tips.

The force on the atom is then given by

$$F_r = \mu_{eff} \nabla_r H_o$$

$$= 2 \frac{\mu_{eff} H_p}{r_p^2} r .$$

For hydrogen, using the Breit-Rabi formula,

$$m_F = 0, \quad \mu_{eff} = \pm \mu_o \frac{x}{(1+x^2)^{1/2}}$$ (here the upper sign is chosen for the F=1 state)

$$m_F = \pm 1, \quad \mu_{eff} = \pm \mu_o .$$

The moment is constant for the $m_F = \pm 1$ states, and for large x values the μ_{eff} of the $m_F=0$ state approaches μ_o. In view of the approximation that is about to be made, it is well to observe that x=1 for a field of about 500 gauss. The field in the hexapole used in practice ranges from zero at the center to over 8000 gauss at the pole tips and therefore putting $\mu_{eff} = \pm \mu_o$ is a good approximation.

$$F_r = \pm kr, \qquad k = \frac{2 |\mu_o| H_o}{r_p^2}$$

Since the force is proportional to the radius, the solution is of the simple harmonic type.

$$r = A \cos \sqrt{\frac{k}{m}}\, t + B \sin \sqrt{\frac{k}{m}}\, t$$

where the force is directed towards axis (atoms in state $F=1$, $m_F = +1, 0$),

and $$r = A' \cosh \sqrt{\frac{k}{m}}\, t + B' \sinh \sqrt{\frac{k}{m}}\, t$$

where the force is away from axis (atoms in state $F = 1$, $m_F = -1$; $F = 0$, $m_F = 0$).

This forms the basis for the calculation of trajectories of atoms from the source to the entrance of the maser bulb and Figure 11 shows the geometry of the problem.

The following method is used to determine the flux into the bulb. The velocities are determined for the trajectories of the atoms that

a) graze the magnet tips and enter the bulb by grazing the upper part of the hole--see trajectory fast (Figure 11);

b) graze the magnet tips and enter the bulb by grazing the lower part of the hole--see trajectory slow (Figure 11).

These are the fastest and slowest atoms that have the largest possible entrance solid angle.

The solid angle of the magnet is given by

$$\frac{\Omega}{4\pi} = \frac{\theta_o^2}{4} = \frac{1}{4} \frac{r_p^2}{\ell_1^2 + \frac{v^2}{\omega^2}} = \frac{1}{4} \frac{\omega^2 r_p^2}{v^2} \qquad \text{(where } \ell_1 = 0 \text{ in this case)}$$

The flux of atoms is obtained by

$$I = \int_{v_{slow}}^{v_{fast}} \pi r_s^2 \cdot \frac{\pi 2 \mu_o H_p}{m v^2} \cdot \frac{2 I_o}{\alpha^4} v^3 e^{-v^2/\alpha^2} dv,$$

$$= \begin{matrix}\text{area of} \\ \text{source}\end{matrix} \times \begin{matrix}\text{solid} \\ \text{angle}\end{matrix} \times \begin{matrix}\text{velocity distribution} \\ \text{of atoms in a beam}\end{matrix}$$

where $$\alpha^2 = \frac{2kt}{m}$$

$$I_o = \tfrac{1}{4} \eta v_a = 3.513 \times 10^{22} \frac{P_{mm}\, cm^{-2} sec^{-1} *}{\sqrt{MT}}$$

η = density in the source

v_a = average velocity

M = mass number.

---

* S. Dushman, Vacuum Technique, p. 17 (John Wiley & Sons, New York).

Then

$$I = \pi r_s^2 \frac{\pi 2 \mu_o H_p}{m} \frac{I_o}{\alpha^2} \left[e^{-v_s^2/d^2} - e^{-v_f^2/d^2} \right] \quad (1)$$

There are some faster and slower atoms that are launched more parallel to the axis and do not graze the magnet; however, due to the strong velocity selectivity of the system, these atoms account for only a very small portion of the beam.

The trajectories are obtained as follows. At a distance ℓ_3 from the exit of the magnet

$$r = r_p \sin \frac{\omega \ell_2}{v} + \frac{\omega \ell_3}{v} r_p \cos \frac{\omega \ell_2}{v} . \quad (2)$$

For $r = \pm r_i$

$$\pm \frac{r_i}{r_p} = \sin \frac{\omega \ell_2}{v} + \frac{\omega \ell_3}{v} \cos \frac{\omega \ell_2}{v} .$$

Solving this for v for both signs of r_2 gives the velocities v_s and v_f.

It is useful to know the trajectory of the center ray $r_i = 0$, and this is given by the solution of

$$\tan \frac{\omega \ell_2}{v} = - \frac{\omega \ell_3}{v} . \quad (3)$$

By choosing a value of v (usually the most probable velocity = $\sqrt{\frac{3}{2}}\alpha$) and the length of beam ℓ_3, the hexapole can be designed if a value of maximum field is given.

As an example, let the source temperature be 300^0K, the magnet radius be 1.59 mm., ℓ_3 = 29 cm., H_p = 8 kilogauss, and $v = \sqrt{\frac{3}{2}}\alpha$. Solving equation (3) for ℓ_2 gives ℓ_2 = 8 cm.

If the hole in the bulb has radius 1 mm., then solving equation 2 for v_{fast} and v_{slow} gives

$$v_{fast} = 1.059 \sqrt{\frac{3}{2}}\alpha.$$

$$v_{slow} = .0952 \sqrt{\frac{3}{2}}\alpha.$$

Substituting these as the limits in equation (1), the No./sec./unit source area/ unit source pressure in mm. Hg is given by

$$\frac{I}{\pi r_s^2 \times P_{mm.Hg}} = 3.34 \times 10^{17} \text{ atoms cm}^{-2} \text{ sec}^{-1} \text{ (mm.Hg)}^{-1}$$

The use of a collimated source will make little change in this calculation if the collimation is such that the entrance solid angle of the magnet is filled. This comes as a result that collimation does not change the flux of atoms per unit solid angle for small solid angles in the axial direction.

If the source pressure is taken as 10^{-2} mm. Hg and desired flux is 2×10^{-13} atoms/sec,* the source diameter is found to be 0.86 mm. In practice, the source collimators are about 1 mm. in diameter (see Fig. 3) and are designed to operate between 10^{-1} and 10^{-2} mm. Hg source pressure.

2.4.2 Design and Fabrication of Magnets

The design of the hexapole follows that given by Christenson and Hamilton,[21] where Alnico V pole pieces are mounted in grooves in an Armco Iron yoke. The grooves are made using a special brooch so that the yoke can be made in one piece. Pole tips of Armco Iron are bolted through the Alnico to the yoke using stainless steel screws. Considerable care is taken before assembly to anneal the pole pieces and then to grind them lightly to their final dimensions. The hexapole magnet is shown in Figure 12.

The magnet is energized by winding alternate sections of the Alnico with 25 turns of No. 16 teflon insulated wire. A $\frac{1}{8}$" iron rod is inserted in the gap to close the magnetic paths. A shot of current, obtained from a d.c. arc welder, provides sufficient magnetization to saturate the system. The field is monitored by using a Hall effect probe across a pair of poles and saturation current can be measured. The actual field at the pole tips is difficult to measure due to the small size of the gaps. However, by using a thin Hall probe one obtains an average over the area of the crystal.

* This is about twice the threshold flux for the masers currently in operation.

THE HEXAPOLE MAGNET

FIGURE 12

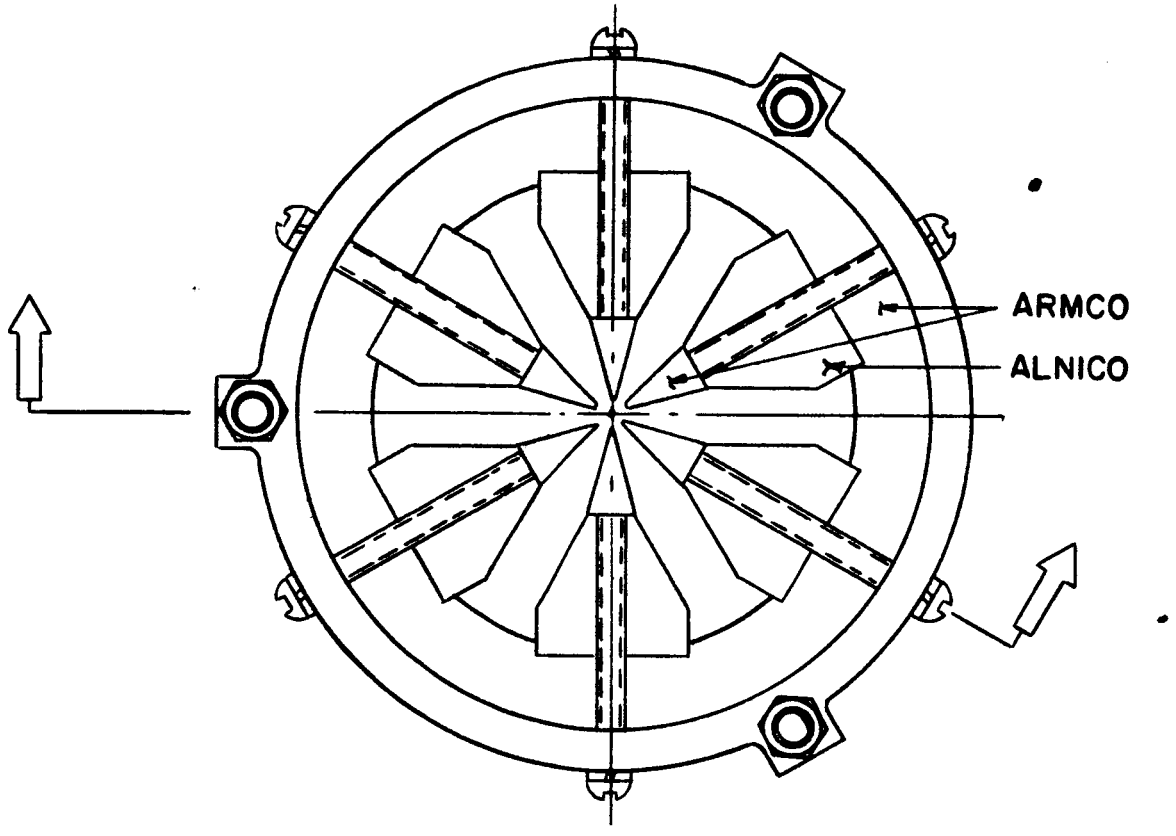

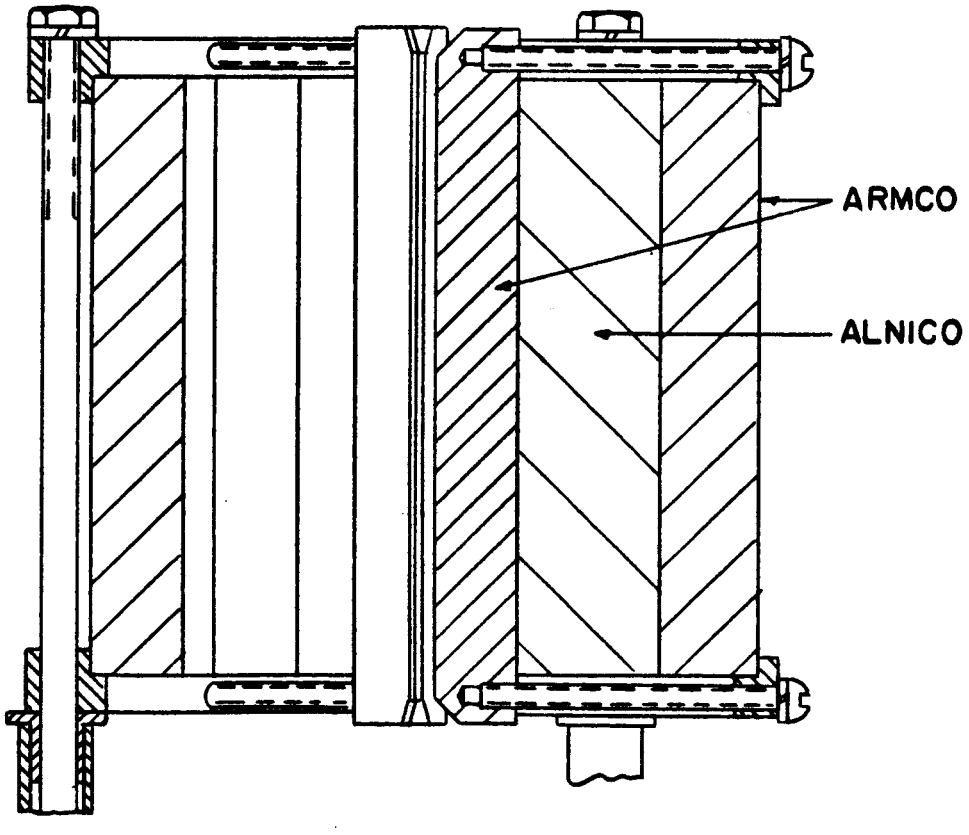

Normally, this reading is greater than 7 kilogauss; however, since it is not possible to determine the effective area of the crystal without destroying the probe, there is considerable uncertainty in this measurement.

A better and more fundamental measurement can be obtained from a coil rotating on the magnet axis and whose windings come close to the pole tips. This is necessarily a small coil and the average effective coil area for a field with a strong gradient is not easily determined; nevertheless, the measurement should be good to 15%. Measurements of several magnets using this technique have shown that the fields are of the order of 8 kilogauss at the pole tips. The signal from the rotating coil should be at 3 times the frequency of rotation, and asymmetries in the field distribution show as signals at the rotation frequency. This serves to check the magnet for uniformity.

2.5 The Storage Bulb

The principal advantage of the hydrogen maser is obtained through the use of a storage bulb having walls coated with a substance that has extremely little effect upon the colliding hydrogen atom. Atoms with average velocities approximately 10^5 cm/sec collide with the walls, rebound and suffer a phase shift with reference to the vector describing the "natural" r.f. precession frequency that can be best described in the following way.

An atom, entering at 10^5 cm/sec into a bulb roughly 10 cm. in diameter, will traverse it about 10^4 times before leaving. In doing so it will have collided about 10^4 times with the walls of the bulb. It has been found experimentally* that the frequency shift under these conditions using teflon walls is a few parts in 10^{11}. This corresponds to an average phase retardation of 10^{-5} radians per collision.

This remarkably small frequency shift is analagous to the pressure shift of gas cell devices but very much smaller. In gas cells the shift is observed to increase or decrease the resonance frequency depending on the type of buffer gas. The decrease in frequency is due to electric fields that

* D. Kleppner, private communication.

arise during the collision, and it can be described as a Stark shift. In cases where an increase is observed, the effect has been described as due to collisions that involve deeper penetration and interaction of the electronic clouds surrounding the colliding atoms. There results from these stronger interactions a confinement of the valence electron of the active atom to a volume that is smaller than normal. From a wave mechanical point of view, since the electron spends more time in the vicinity of the nucleus it has a higher energy of interaction and hence a higher frequency.

The hydrogen interaction with various walls has been measured for two substances, namely dimethyl dichloro silane (drifilm) and tetra fluoro-ethylene (teflon). Both these have shown negative shifts. It is very important that more study be devoted to these shifts and that various types of coatings be investigated and catalogued. It is very likely that a coating can be found that will show far less shift than presently observed for teflon. Experiments will soon be in progress to measure a series of substances.

There are two stages to this determination of wall shift. The first is to verify that the substance in question will not cause relaxation on collision. For this purpose special bulbs have been made having a large opening at the end opposite the entrance hole and coated internally with teflon. The large hole will be closed with a plate made of, or coated with, the sample, and the maser then operated. Frequency shift measurements will not be made using this bulb, as the surface in question is not large enough.

Having found that a particular coating does not relax the hydrogen atoms, the second stage of the experiment consists of coating or manufacturing a bulb of standard dimensions and time constant and operating the maser to compare against others having a standard coating to obtain the relative shift.

The absolute shift is obtained from a series of measurements of bulbs having different diameters to obtain different collision rates (the velocity of the atom is assumed to be that for thermal equilibrium with

the bulb). By varying the collision rates, the shift in frequency can be extrapolated to zero rate giving information about the zero collision resonance frequency as well as the phase shift per collision.

2.5.1 Bulb Coating Techniques

The application of the coating to the bulb should be done in as well controlled a manner as possible to assure reproducible results. So far only three types of coating have been used--dimethyl dichloro silane, tetrafluoro ethylene (T.F.E.),* and fluoro ethyl propylene (F.E.P.).* The last two belong to the "teflon" family, the former having a high melting point and the latter being fusible.

Coatings with drifilm are chemically bonded to the substrate of silicon and oxygen probably through the OH groups that are bound to the quartz surface. The hydrogen combines with the chlorine of the drifilm and is evolved as $HC\ell$ leaving the silicon atom bonded by the vacated oxygen bond. In effect the drifilm becomes an extension of the quartz (SiO_2) surface.

To apply the drifilm, the following procedure is used. First the bulb is cleaned in a chromic and concentrated sulphuric acid bath and rinsed carefully in distilled water. The bulb is then dried in air and equipped with a tube leading to its center through the beam aperture. Argon gas is filtered and bubbled through the liquid dimethyl dichloro - silane and made to enter the bulb. The gas that emanates from the bulb is monitored, and by estimating the size and number of bubbles, one complete change of atmosphere in the bulb is made using the saturated argon. The bulb is now placed on a well trapped mechanical forepump and evacuated. This evaporates the drifilm that is not bound to the quartz. The bulb is now ready for installation.

Bulbs to be coated with drifilm generally have integrally made apertures that control the bulb time constant. Bulbs that are to be coated with teflon use stoppers made of solid teflon with suitably bored holes to provide an aperture having the desired collimation.

---

* T.F.E. Teflon, and F.E.P. Teflon are duPont products.

Coatings of teflon are applied from the water dispersion of T.F.E. or F.E.P. teflon resin. These have roughly 50% solids with water and a wetting agent added. It has been the practice in this laboratory to roughen the inside of the bulb by agitating a mixture of clean glass shot and carborundum. By providing such a surface it is believed that the adhesion of the teflon is improved.

The resin is generally diluted 2:1 with water and a few cubic centimeters of it are very carefully introduced into the bulb using a pipette to avoid making bubbles. The bulb is carefully wetted all over by revolving it and then placed in a rack to allow the excess resin to drain through the stem. Curing of the teflon is done under vacuum and at temperatures up to 475°C in the following way. The bulb is installed on a vacuum stand consisting of a liquid nitrogen cooled trap and a mechanical forepump. A low temperature bakeout at 150°C is used to drive off the wetting agent, and this temperature is maintained for about 10 minutes. The bulb is then raised to 450°C to 475°C as measured on the bulb surface by thermocouples, and the teflon is observed to fuse into a relatively smooth film.

A rudimentary check of the coating can be made by putting a drop of water into the bulb and observing it roll around. If the water sticks to the surface anywhere, it is a sign that the coating has a flaw.

It has been observed that the coating thickness or uniformness has no effect on the maser and that fairly heavy coatings, fused in this manner under vacuum, do not outgas appreciably when installed in the maser, and no bakeout of the bulb is necessary.

2.6 The R.F. Cavity

Of all the sources of instability that presently beset atom beam resonance devices, the cavity or r.f. structure is the most troublesome. In the case of the hydrogen maser, the detuned resonance frequency of the cavity will "pull" the oscillating frequency of the transition. Similarly in the case of the r.f. structure on beam resonators, an asymmetry in the

phase of the r.f. coupling can result in a pulling of the resonance frequency. For devices such as the hydrogen maser where the line Q is larger than the cavity Q, this expression has the form

$$(\omega - \omega_o) = (\omega_{tuned} - \omega_o) \frac{Q_c}{Q_\ell}$$

where Q_c is the loaded Q of the cavity and

Q_ℓ is the line Q of the atomic transition. (In hydrogen masers, $Q_\ell = \frac{\omega_o}{2\gamma}$ where γ^{-1} is the storage time constant of the bulb.)

The cavity Q also plays a role in the threshold level of flux for oscillation.

$$I_{th} = \frac{h V \gamma^2}{8\pi^2 \mu_o^2 Q \eta}$$

where h is Planck's constant,

V is the volume of the cavity

γ is the bulb relaxation time constant

μ_o is the Bohr magneton

Q is the loaded quality factor of the cavity

η is the ratio $\frac{\langle H_z^2 \rangle_b}{\langle H_{rf}^2 \rangle_V}$

H_{z_b} is the component of r.f. magnetic field parallel to the d.c. field in the bulb.

One can gain in insensitivity to cavity tuning by diminishing the loaded cavity Q by decreasing the value of γ for a given flux level. The term γ, however, consists of many relaxation constants such as exit time constant, γ_b, wall quenching, γ_ω, spin exchange, γ_{se}, and the effect of impurity gases, γ_{imp}.

$$\gamma = \gamma_b + \gamma_\omega + \gamma_{se} + \gamma_{imp}$$

Of these, at low flux intensities the most important is the value of γ_b which normally is made about 3 sec^{-1}. The value for γ_{se} depends on the pressure in the system and for normal operation is usually about 0.5 sec^{-1}.

Typical values used at present are

$$Q_c = 4 \times 10^4$$
$$Q_\ell = 14 \times 10^9$$

so that for a fractional frequency stability of a few parts in 10^{13} the cavity must remain tuned to within 5 cycles/sec.

In the first masers the bulb formed part of the vacuum envelope and the cavity, surrounding the bulb, was open to the atmosphere. Changes in barometric pressure and in humidity will alter the dielectric constant of the air in the cavity sufficiently to detune the cavity. A simple solution to this problem is to enclose the cavity in the upper vacuum system. Other advantages are also realized due to simplification in the bulb mounting as well as in thermal control. The cavity and bell jar vacuum envelope are shown in Figure 13.

To achieve the necessary stability against thermal and mechanical variations, considerable attention was devoted to the structural design of the resonator. In a relatively quiet environment where no large shocks or accelerations are expected, the mechanical flexure problem is not difficult to solve and the primary concern is thermal movements. One can cope with the problem by reducing the thermal variability of the cavity and by stabilizing the environment of the cavity so that thermal fluctuations are very small. These methods are now in use. Temperature compensation of a cavity can be obtained in several ways, and considerable simplification results from the fact that the cavity is used over an extremely narrow band of frequencies.

The present cavities are cylindrical in form and operate in the circular E mode that presents a reasonably large volume of uniform r.f. magnetic field. By using a hollow silvered quartz cylinder having a low expansion coefficient, gross thermal detuning can be avoided. The residual detuning can be compensated by mounting one of the ends on metal posts that expand inward as the walls expand radially outward (see Figure 1). For an unloaded

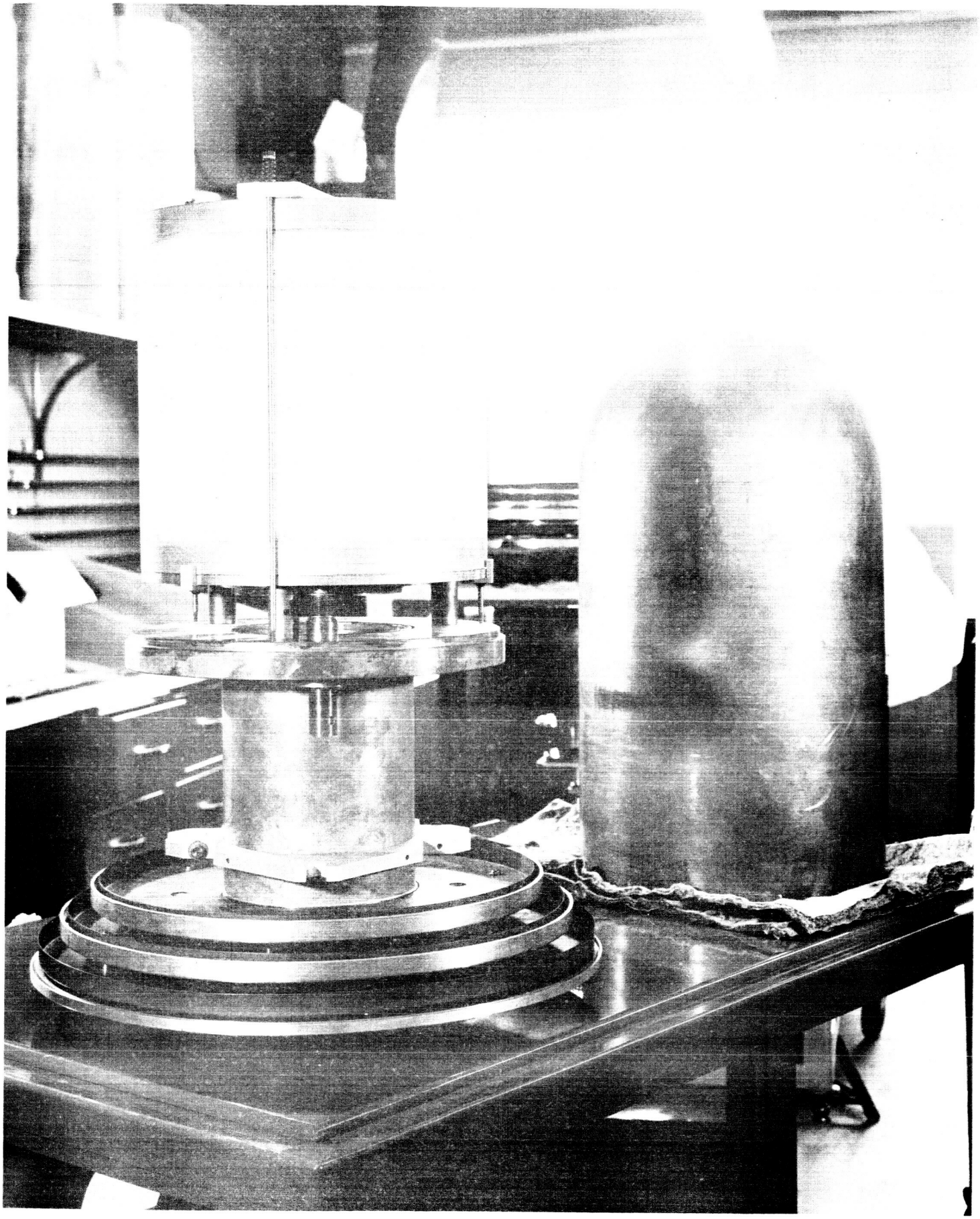

Figure 13

cavity, the calculation is relatively simple. However, for the present configuration involving a quartz bulb, the problem is somewhat different. The important parameter is the tuning rate in megacycles per cm. of motion of the end plate. Measurements have shown that the cavity length must be changed from 27.9 cm. to 24.1 cm. in order to stay in resonance when a typical bulb is introduced. The tuning rate for the loaded cavity has been measured and was found to be very nearly that of an unloaded cavity having the loaded cavity dimensions.

For compensation we need the sum of all thermal frequency shifts to equal zero.

$$\left.\frac{\partial \nu_r}{\partial T}\right|_{\ell} = \frac{\partial \nu}{\partial r}\,\frac{\partial r}{\partial T}\,, \quad \text{the radial thermal tuning rate,}$$

$$= \frac{\partial \nu}{\partial r}\,\alpha_q\, r_q \quad \text{where } \alpha \text{ is the linear coefficient of expansion of the quartz,}$$

r_q is radius of quartz cavity,

$$\left.\frac{\partial \nu}{\partial T}\right|_{r} = \frac{\partial \nu}{\partial \ell}\,\frac{\partial \ell}{\partial T}\,. \quad \text{the axial thermal tuning rate.}$$

$\frac{\partial \ell}{\partial T}$ is made of two parts--an elongation of the quartz and an elongation of the compensating posts.

$$\frac{\partial \ell}{\partial T} = \frac{\partial \nu}{\partial \ell}\,(\alpha_q\,\ell_q - \alpha_p\,\ell_p) \quad \text{where } \alpha_p \text{ is the linear coefficient of expansion of the compensating posts,}$$

ℓ_p is the length of the posts.

For compensation:

$$\left.\frac{\partial \nu}{\partial T}\right|_{\ell} + \left.\frac{\partial \nu}{\partial T}\right|_{r} = 0$$

$$\frac{\partial \nu}{\partial r}\,\alpha_q\, r_q + \frac{\partial \nu}{\partial \ell}\,(\alpha_q\,\ell_q - \alpha_p\,\ell_p) = 0$$

$$\alpha_r\,\ell_r = \alpha_q \left[\frac{\frac{\partial \nu}{\partial r}}{\frac{\partial \nu}{\partial \ell}}\, r_q + \ell_q\right] .$$

Since ℓ is determined by the length of the quartz and the degree of the detuning due to the load, and α is given by the nature of the materials, it is often necessary to use two materials having different α's such that

$$\alpha_p \ell_p = \alpha_1 \ell_1 + \alpha_2 \ell_2 .$$

Fine tuning of the cavity is done by means of a small plunger entering the lower end plate of the cavity actuated through the vacuum envelope by means of bellows and adjusted by a finely threaded positioning nut. (See assembly 52 to 60 inclusive, Figure 14.) Coarse tuning during assembly is obtained by etching the compensating posts (42) (43) of Figure 14.

Thermal compensation as described here is affected adversely by thermal gradients and care must be taken to keep the temperature of the cavity as uniform as possible. This topic will be discussed in the following section.

2.6.1 Thermal Control

In the previous section a description of the technique for thermally compensating the resonant frequency of the cavity was described. It is necessary to reduce temperature gradients as much as possible for this technique to be successful. A further large gain in frequency stability is realized by controlling the temperature. The cavity is enclosed in two concentric cylindrical ovens. Each oven consists of bifilar heater coils wound on an aluminum cylinder capped at both ends. (See 4, 28, 29, 45, 47 and 67, Figure 14.)

The cylinder and caps form an isothermal enclosure. Between the outer and inner oven there is an insulated gap 1 inch in thickness filled with glass fibre (17). The outer oven is similarly insulated. The inner oven and bell jar are in good thermal contact using copper tube pellets (20), and the bell jar (33) forms a second thermal equipotential. Heat conduction to the cavity from the bell jar is provided by three copper mounting studs (14) to the cavity base (16) and by three silicon bronze rods (21) to the cavity top and compensating system (19, 37, 39, 42, 43). There are numerous

undesirable paths for heat conduction such as between the ovens at the mounting spacers (1, 2, 3, 82) and these spacers are made of thin stainless steel tubing to minimize the effect. Major heat leakage paths such as the r.f. coupling (76, 15) and tuner mechanisms (60) are tied thermally to a thermal reference plane (74, 75) clamped at the base of the neck. The temperature difference across the copper neck (62) between this plane and the base plate of the bell jar (13) is determined by a 10 junction thermopile with a sensitivity of 600 $\mu V/^0C$ and used to servo a heating coil bifilar wound at the base of the thin stainless section (70). An auxiliary control winding is also located at this point and its function will be described below.

Temperature sensing for servo control of inner and outer ovens is done by platinum bridges located on the aluminum oven cylinders midway between top and bottom. A separate bridge for monitoring is located at the bell jar base. As the excitation for the bridges must be floating with respect to ground due to the desirability of having unbalanced inputs to the servo amplifier, a floating 0.8 V excitation supply has been made using two photo cells illuminated by a tungsten bulb. This supply is well shielded and very constant. The outputs from the bridges have a temperature sensitivity of 1.6×10^{-3} $V_o/^0C$ and are led to chopper stabilized amplifiers which control the heater current. The gain of the system as given by $T_{out} \Delta T_{in}$ is approximately 100.* The circuits for these amplifiers are shown in Figure 15.

Heater power from the outer oven servo amplifier is also applied to the auxiliary winding on the neck and provides heat to compensate that lost to the outside of the maser.

The time constant of the response to the transient temperature shift for the inner oven is about 2.6 hours, and the control under normal room temperature range is such that the temperature monitored at the bell jar base is held to within $\pm$ 0.014^0C.

---

* Note: Limited by leakage paths and not servo gain.

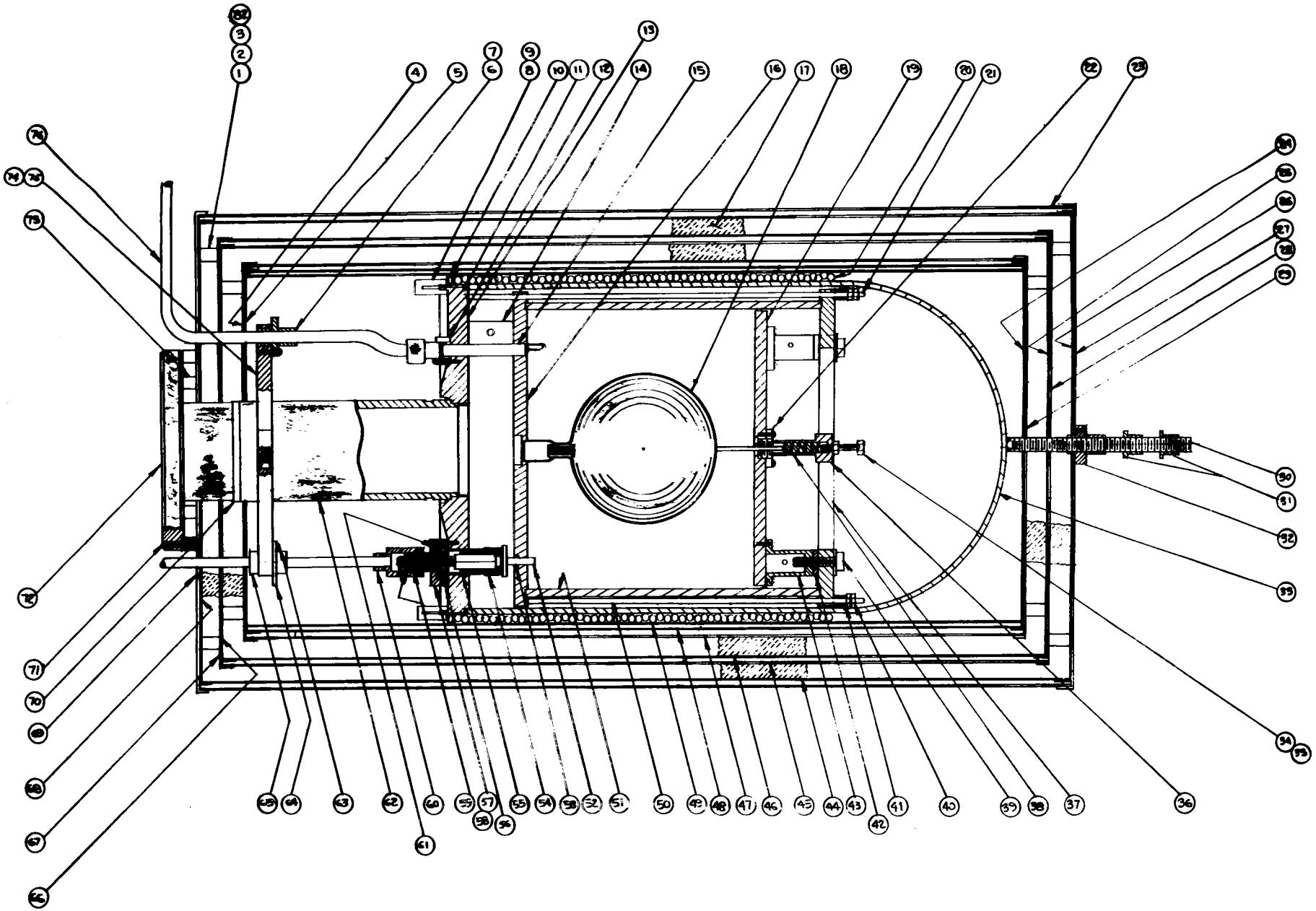

Figure 14

INNER AND OUTER OVEN THERMAL CONTROL SYSTEM

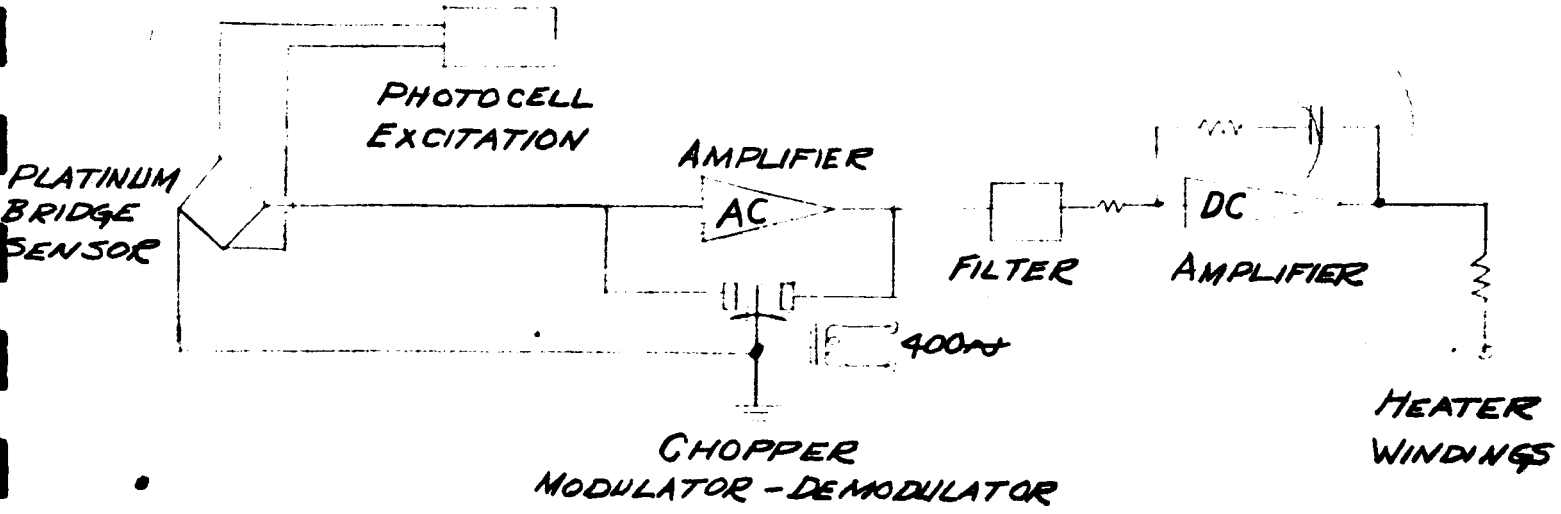

A-C AMPLIFIER - FILTER

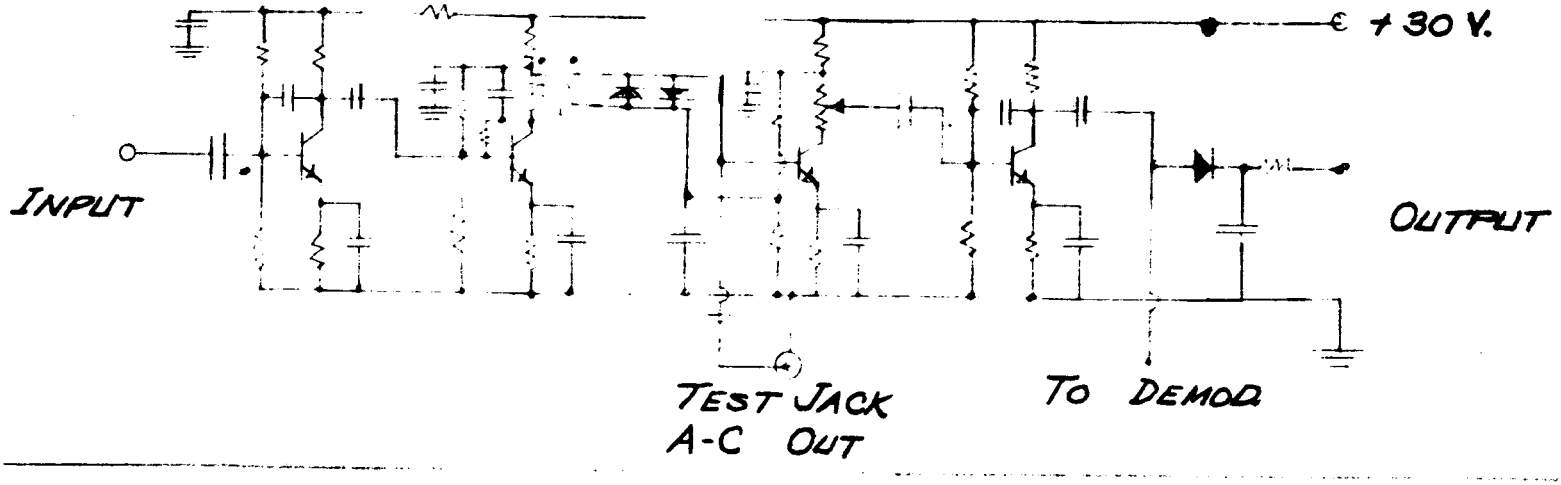

D-C AMPLIFIER - INTEGRATOR

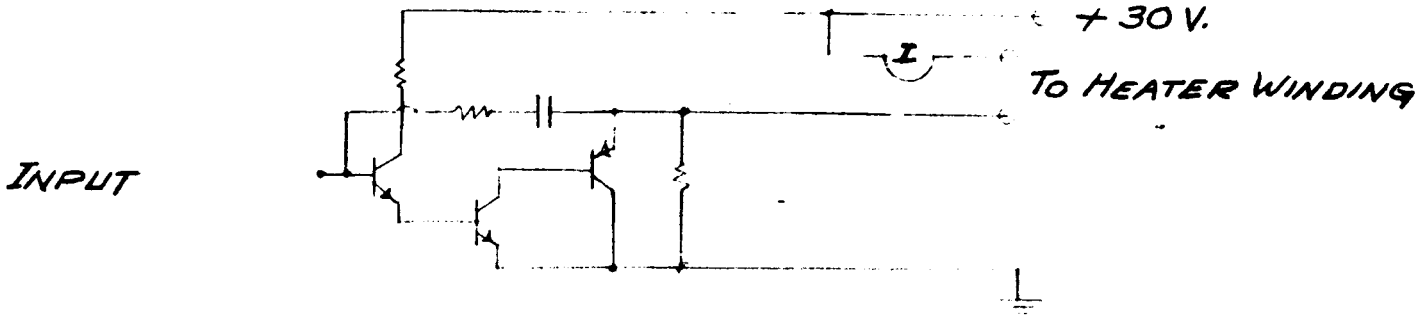

FIG. 15

2.7 Magnetic Shielding and Field Controls

The requirements for magnetic shielding and control of the residual magnetic field are best understood by considering the Breit-Rabi formula

$$W(F,m) = -\frac{\Delta W}{2(2I+1)} - \frac{\mu I}{I} H_o m \pm \frac{\Delta W_o}{2}\left[1 + \frac{4m}{2I+1}x + x^2\right]^{\frac{1}{2}}$$

For the transition $F = 1,\ m_F = 0 \rightarrow F = 0,\ m_F = 0$ of atomic hydrogen, the energy difference $\Delta W = h\Delta\nu$ is given to second order in x by

$$\Delta\nu \doteq \Delta\nu_o + \frac{\Delta\nu_o x^2}{2}$$

$$\Delta f = \Delta\nu - \Delta\nu_o = 2750 H_o^2$$

Δf is the frequency shift due to the presence of the magnetic field in the bulb. The shift is quadratic in H_o and for the case of the hydrogen maser where an atom occupies, on the average, all the space inside the bulb, the average of H_o^2 must be taken in calculating Δf.

Gradients in the bulb can produce relaxation of the excited states in several ways. If the field in the bulb is very small and has gradients, it is possible for Majorana transitions to occur due to motion of atoms in the spatially varying field which appear as time-varying fields to the atom. Transitions occur when the component of r.f. thus generated is sufficiently strong in the frequency range associated with the transition. These transitions involve changes ± 1 in the m value of the upper energy state.

A second "relaxation" involves the phase decorrelation of atoms as they spend their time in fields of varying intensity. A spread in the phase of the oscillating magnetic moments of atoms occurs when the atoms wander about in regions of higher and lower d.c. magnetic fields. This effect is more pronounced at higher fields and, for the $F = 1,\ m_F = 0 \rightarrow F = 0,\ m_F = 0$ transition, arises from the quadratic behavior described above as $\Delta f = 2750 H_o^2$.

The control of frequency against field fluctuation is best achieved at low fields as shown below.

$$d\Delta f = 5500 H_o\, d H_o$$

If the uniform field is produced by a solenoid, then H_o will be proportional to I and

$$d\Delta f = 5500\, H_o^2 \frac{dH_o}{H_o}$$

$$= 5500\, H_o^2 \frac{dI}{I}.$$

Given $\frac{d\Delta f}{f} = 10^{-13}$ and $H_o = 10^{-3}$ oersteds, then

$$\frac{dI}{f} = \frac{10^{-13} f}{5.5 \times 10^{3} \times 10^{-6}} = 2.5 \times 10^{-2}.$$

This degree of current stabilization is not difficult to obtain.

2.7.1 Magnetic Shielding

The problem in magnetic field control is that of removing the ambient field and replacing it with one that is uniform. The shields will play two roles in this effort. First, they reroute the externally applied field lines away from the interior. Second, the inner shield forms a cylindrical equipotential surface for the fields generated by the interior solenoid.

When the solenoid windings are brought right up to the end caps, the currents and their magnetic images will produce the effect of an infinite solenoid and provide a very homogenous magnetic field.

The effectiveness of the shield depends upon the magnetic permeability of the material from which it is made. In the case of an infinite cylinder of radius b and thickness t, the shielding factor G can be given very closely by

$$G = \frac{\mu}{2} \frac{t}{b}.$$

For two concentric cylindrical shields where the spacing between them is large compared to the radius

$$G = \frac{\mu^2 t^2 s}{2\, b^3} \qquad s >> b\ .$$

The progression from one to two shields indicates that the spacing is as important as the thickness. More important, however, it is seen that the shield factor depends on the permeability raised to the power n where n is the number of shields. Shielding materials such as mu metal* are described as having permeabilities in the 10^4 to 10^5 range and therefore, typical double shields should have shielding factors of about 10^4. The interior fields for an exterior ambient field of one gauss would then be 100 microgauss. Unfortunately, there are other properties of the metal that deteriorate this performance considerably. At low fields (tens of milligauss and less) the permeability is less high, but more serious is the question of remanence or permanent magnetization that may be present in certain areas of the shield. These are removed by degaussing the shield by the usual technique of using a slowly diminishing a.c. field. However, an improperly annealed shield will have "hard spots" where the coercive force and remanence may be high and the shielding effect for a small change of field will be poor.

Due to the quadratic nature of the magnetic dependence with frequency at low fields, it is desirable to operate the device at as low a field as possible to minimize the effect of field fluctuations on the output signal. It is important to consider the effectiveness of the magnetic shielding before setting a magnetic field intensity at which to operate. Fluctuations in the external ambient field due either to terrestrial or local causes will be shielded out of the interaction region by a factor, S, which depends on the nature of the shields. The internal field change is 1/S times the internal field change

$$\Delta H_{o_{int}} = \frac{1}{S} \Delta H_{o_{ext}}$$

The level of field at the bulb chosen for operation must be greater than the largest $\frac{\Delta H_{o_{ext}}}{S}$ expected in order to avoid gradients large compared to the average field in the bulb and the consequent Majorana transitions.

Triple shields consisting of concentric μmetal cylinders having the following dimensions have been used.

---

* Allegheny Ludlum Steel Corporation, Brackenridge, Pa.

	Length	Diameter	Thickness of Metal
Inside	32"	15"	0.025"
Center	34"	17"	0.025"
Outside	36"	19"	0.032"

The incremental shielding factor S for changes of $H_{o_{ext}}$ of 0.05 gauss has been measured and found to be between 190 and 250. The factor based on calculations involving the low field permeability of mu metal is very much greater. However, little data on incremental permeability at very low fields is available and it is likely that other materials such as moly permalloy may be superior in performance.

The shielding problem is one which might be broken down into two parts. The first problem would be to obtain shields that will reduce the external ambient field from 1 gauss to 0.01 gauss regradless of the orientation of the shield in the external field. The second part of the problem is to construct an inner shield having very good incremental shielding factors that would operate in the low field environment created by the outer shield.

At present the shields exhibit some residual magnetism and must be degaussed while in the ambient field of the place where the maser is located. The process is really not one of demagnetizing the shields but rather one of realigning the ferromagnetic domains of the shields to the position of least energy with the ambient field. Unfortunately these domains still require energy for their realignment and this is supplied by the usual method of applying an alternating magnetic field that gradually is diminished to zero. The emphasis on the design of very low field shields should not be placed on high mu materials; it should be placed on having low coercive force. If a given material does not have both properties, then a composite system should be built.

An important local cause of field perturbation results from the magnets used on the two VacIon pumps mounted on the maser. The problem of shielding the static field is not serious since the existing triple mu metal shields, properly degaussed, will provide fields low enough for maser operation. However, since

these external magnets are strong, the external static field can be varied easily by the presence of magnetic materials moving nearby that change the reluctance of the magnetic paths. These effects are minimized by housing the magnets in shields consisting of two layers. The inner layer is made of 0.007" permalloy and is spaced at least 2 inches from the magnets. The outer layer, spaced one inch from the inner layer, is made of 0.032" mu metal. Both magnets are housed in the same enclosure and are oriented so as to present a small total dipole moment.

2.7.2 Degaussing Techniques

Several methods for degaussing shields have been tried, and these will be briefly reported.

The first method used was to wind a degaussing coil about each shield and separately energizing it from a variable transformer. Sixty-cycle alternating current was applied so as to saturate magnetically the mu metal and the current was then reduced slowly to zero. Each shield in turn, from the outside in, was degaussed. Besides being cumbersome, this method had the disadvantage of not effectively degaussing the end caps of the cylindrical shields.

A second method was tried which involved winding a coil toroidally about each shield, threading the wire through the inside and around the outside. Caps were wound in the same manner by passing the wire through a small center hole in the case of the upper cap or through the hole for the mounting neck in the case of the lower cap.

Each piece had a one-turn pick up coil used to display the saturation and monitor the process on an oscilloscope. In all cases a magnetomotive force of less than 500 ampere turns was necessary to obtain saturation. Degaussing using this process was more satisfactory than previously, although the technique was more complicated.

Simplification of the method was obtained by passing 500 amperes through a one-turn coil that threaded all the shields. This "coil" consists of the conducting

bell jar and an insulated terminal on the top of the shields. The connection is made as shown in Figure 1. A copper bar is threaded in an insulating bushing and tightened so as to contact the top of the jar. High current connections are made to the bar and to a lug at the base of the neck, and lead to a low voltage, high current transformer fed by a variable transformer. The power required is moderate and readily controlled by a 1.5 KVA variable transformer.

2.8 Magnetic Field Measurement

The importance of the magnetic field stability has been described and the necessity of making accurate measurements is quite obvious. If one considers the energy level diagram (Figure 10), it will be observed that the upper energy level designated as $F = 1$ is a triplet state and its degeneracy is resolved into three components when a magnetic field is applied. Transitions can be made from the $m_F = 0$ level to both the $m_F = +1$ and $m_F = -1$ levels, and at low field, the transition frequency is given by $\Delta f = 1.4 \times 10^6 H$ cps. By observing the level of oscillation of the maser while these transitions are being made, it is possible to resolve the applied frequency to better than one cps, which gives a precision to the measurement of better than 7×10^{-7} gauss. In view of the long resonance interaction time of the hydrogen maser, it is potentially an outstanding magnetometer. Operated as a maser using the field dependent transitions, the output frequency will represent the center of the narrow line resonance in a manner equivalent to dividing the line into many thousand parts. Measurement of field variations accurate to 10^{-11} gauss should thus be possible.

Included in the maser is a Helmholtz coil located immediately outside the cavity and oriented to produce an alternating magnetic field transverse to the d.c. field as prescribed by the selection rules for $\Delta m_F = \pm 1$ transitions. These windings are not grounded to the apparatus. To do so would make possible Seebeck effect currents from a warm junction of dissimilar metals inside the bell jar and a cooler junction in the room. These currents through the Helmholtz array will cause spurious fields in the cavity.

Power from a variable frequency oscillator at 50 ohms impedance is fed through a set of attenuators to a step-down transformer, the output of which is connected to the Helmholtz coils. To make a measurement, the maser output power level is monitored by observing beats against another oscillator. A signal at high level is applied and scanned in frequency until the oscillation of the maser is seen to be quenched. Power to the coils is reduced and finer adjustment of frequency is made until the desired level of accuracy is achieved. Care should be taken to be sure that the resonant frequency is not a second or higher harmonic of the signal generator. It is often found that some generators are quite rich in harmonics. A simple check can be made by doubling and tripling the oscillator frequency.

3.0 MEASUREMENTS AND DATA FROM HYDROGEN MASER EXPERIMENTS

3.1 Introduction

The experimental program at Varian Associates, Bomac Division, has been in progress since December 1960. Support from the Office of Naval Research was obtained in September 1961 which was directed toward the research and development of hydrogen masers. In February 1962 Varian, Bomac, contracted with the National Aeronautics and Spece Administration to construct two state-of-the-art- masers. These were built using the best techniques known at the time and are shown in Figure 16. A cooperative effort between NASA and the navy resulted in measurements made on the NASA masers via V. L. F. transmissions and Loran "C" against standards monitored by the Naval Observatory in Washington.

In the following section, data will be reported from measurements of the relative stability of these two masers as well as their stability as measured via external communications. The external data was submitted daily to Dr. William Markowitz of the Naval Observatory. The data was reduced and the numerical calculations were then worked out and the numbers later reported back to the Varian Associates laboratory at Beverly, Mass.

A report by Dr. Markowitz is given in Appendix I describing the results of this comparison.

3.2 Measurements and Data

The hydrogen maser has the outstanding characteristic of being able to confine atoms in a relatively small volume for periods of time many seconds in duration without appreciably perturbing the atoms as they interact with an electromagnetic field. This long interaction time results in a very narrow resonance that can be described as having a line Q, Q_ℓ, equal to

$$\frac{\omega_o}{2\Delta\omega_r} = \frac{\omega_o}{2\gamma}$$

where γ is the storage time constant for atoms in the volume of interaction

with the r.f. field. The atoms enter the interaction region in an upper hyperfine state and are stimulated to make transitions to the lower hyperfine state.

If the power emitted by the atoms exceeds the losses coupled to the r.f. field, then the system will oscillate continuously at the frequency near the center of this narrow resonance. In the presence of the thermal noise in the cavity, the r.m.s. fractional frequency deviation for a measurement made in a time interval T_{obs} is given by[24,25,26]

$$\frac{(\Delta\omega^2)^{\frac{1}{2}}}{\omega_o} = \frac{0.113}{Q_\ell}\sqrt{\frac{kT}{P_b T_{obs}}}$$

where K is Boltzmann's constant,

T is the absolute temperature, and

P_b is the power delivered by the beam to the cavity.

In this expression only the effect of thermal noise is considered. Other effects on stability such as cavity detuning, magnetic field fluctuation, changes in the wall interaction, shifts due to pressure effects such as spin exchange processes and changes in second order Doppler effect can be described in other ways.

3.2.1 Cavity Tuning

The effect on frequency of cavity tuning is described by

$$\frac{\omega - \omega_o}{\omega_o} = \frac{\omega_c - \omega_o}{\omega_o}\,\frac{Q_c}{Q_\ell}$$

where ω is the emitted frequency

ω_o is the resonant frequency of the atom under the conditions prevailing in the maser.

For operation under the conditions described below and in order to achieve fractional frequency shifts less than 10^{-13} the cavity must stay tuned to within 5 c.p.s.

$$\Delta fr = 10^{-13} f \frac{Q_\ell}{Q_c} \doteqdot 5 \text{ c.p.s.} \qquad \begin{aligned} Q_\ell &= 1.4 \times 10^9 \\ Q_\ell &= 4 \times 10^4 \end{aligned}$$

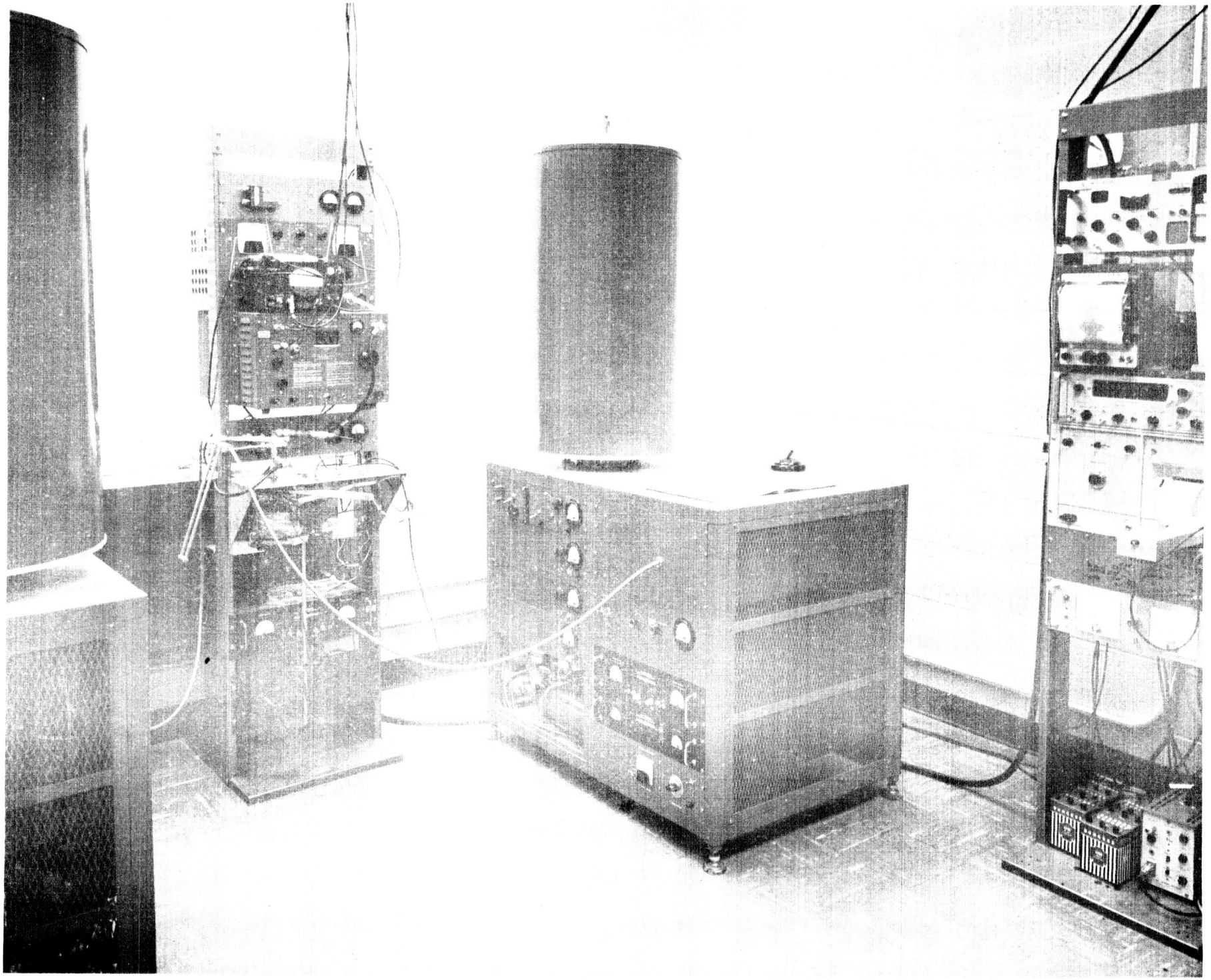

Figure 16

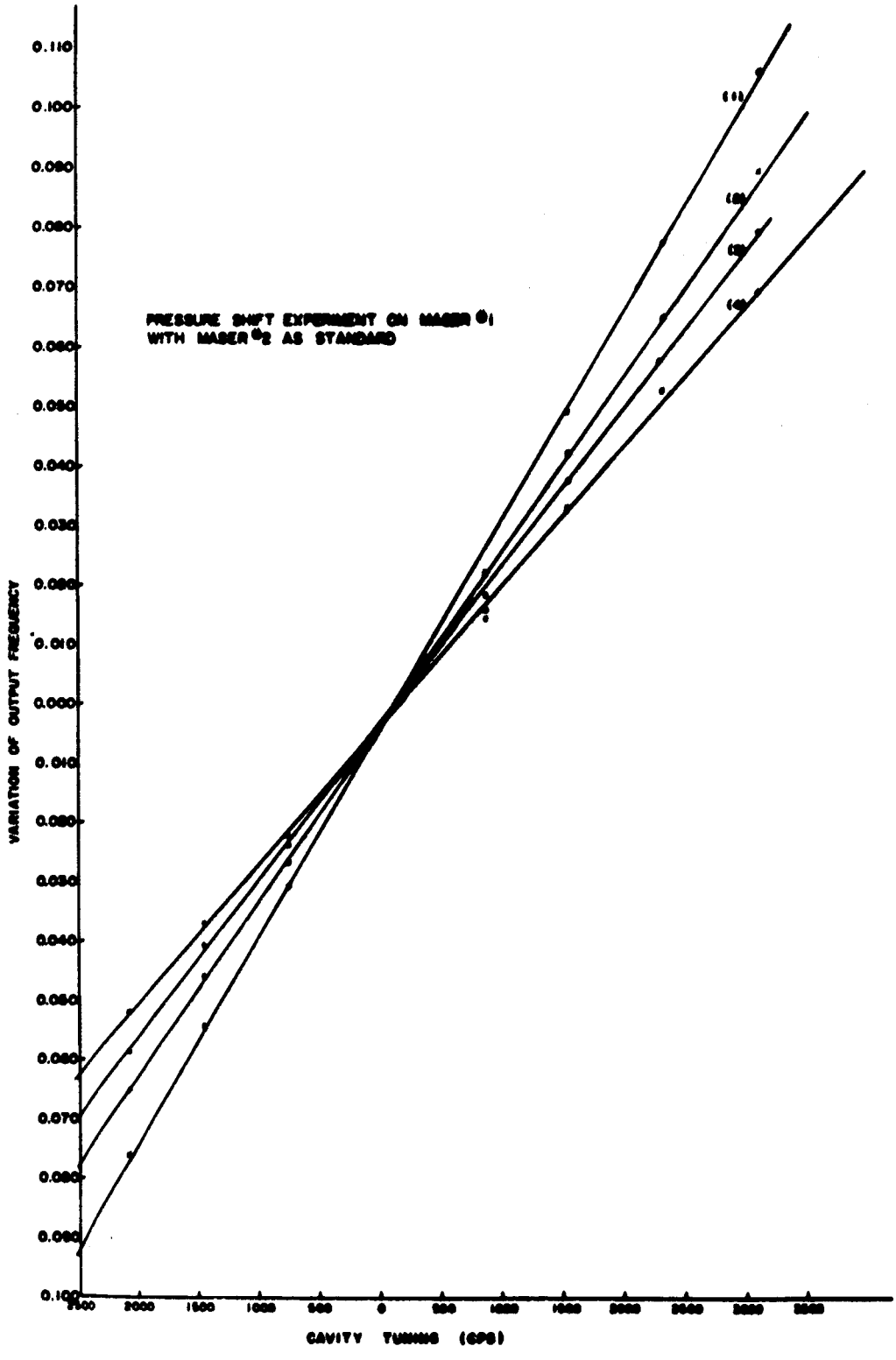
PRESSURE SHIFT EXPERIMENT ON MASER #1
WITH MASER #2 AS STANDARD
VARIATION OF OUTPUT FREQUENCY
CAVITY TUNING (CPS)

Figure 17

Cavity tuning currently is achieved by varying the line Q using spin exchange relaxation processes that result from increasing the flux into the storage volume. A factor of two change in Q_ℓ can be obtained (see Figure 17). To set the maser to the resonant frequency of the hydrogen atom while in the bulb, the cavity is tuned by comparing the maser being tuned with another maser running at a constant rate. The second maser need not be in tuned condition. The pressure of the source is varied and the cavity is adjusted so that no shift in the beat frequency is observed. The resettability is found to be as accurate as the ability to measure the relative frequency; it is limited by the noise of the receiver and the relative stability of the masers during the measuring time. Currently one can, by this method, independently reset two masers such that the fractional frequency difference is less than 8 parts in 10^{13}.

For coupling the maser to a receiver or other device, it is important that the impedance seen by the output coupling from the maser cavity be constant. An isolator is placed in the coupling line to prevent changes in the line termination from changing the resonant frequency of the cavity. In a receiving system involving more than one maser the isolation is also needed to prevent the locking of one maser to another.

3.2.2 Magnetic Field Variation

Effects of magnetic field on the $F = 1$, $m_F = 0$; $F = 0$, $m_F = 0$ transition can be represented by

$$\nu - \nu_o = 2750\ H^2$$

and to hold the fractional frequency shift to one part in 10^{13} requires that a field of 10^{-3} gauss be held constant to 3%.

It is possible to operate the masers at fields less than 0.088 milligauss by carefully degaussing the shields using a large a.c. current passing axially through the three concentric shields. The shields are saturated at about 500 amperes and the current is slowly diminished to zero. The leakage of flux through the hole is offset by a small coil at the bottom of the Z field solenoid.

Since the incremental shielding factor, $S = \frac{\Delta B \text{ outside}}{\Delta B \text{ inside}}$, is only about 200 for the present shields, it is well to operate at about 1 milligauss to avoid field reversal at the bulb due to changes in the ambient field in the laboratory.

The average magnetic field in the bulb is measured using the Zeeman transitions $\Delta m_F = \pm 1$ in the $F = 1$ state of atomic hydrogen. Transitions are detected by a dip in the amplitude of the output signal. Measurements can be made well within ± 1 c.p.s. or $\pm 7 \times 10^{-7}$ gauss.

The Zeeman frequency of the masers has been measured periodically and it has been found to vary less than 5×10^{-5} gauss.

3.2.3 Measurements

Frequency comparison measurements between the two masers have been made by putting both maser signals into a single receiver consisting of a mixer and i.f. amplifier terminated in a diode. The output of the diode is filtered and fed to a strip recorder. In order to get a fast read-out of period measurements for tuning purposes as well as for making short term stability measurements, the frequency of one maser is shifted by increasing its Z axis field by a known amount. The signal is amplified and fed to a recorder for monitoring and to a period measuring counter operating a digital-analog converter where the last significant digits are either printed or traced on another recorder. This circuit is shown in block form in Figure 18.

Measurements of long term stability are now in progress. Figure 19 shows the manner in which the data is recorded, and Figure 20 is a plot of the fractional frequency stability of a pair of masers that have been operating for 7 days. There is evidence that several times the masers locked together (see A, B, C, D, Figure 19 and Figure 20). Consequently, at 11 a.m. on February 2 the magnetic field was further offset (see E, Figure 19 and 20) and thereafter the beat was steady. A histogram of the data taken at hourly intervals for the five days that followed is shown in Figure 21. The histogram shows two peaks and, as seen from the data, there is a diurnal fluctuation of about 5×10^{-13}. It is more likely that there is a temperature effect here than a mag-

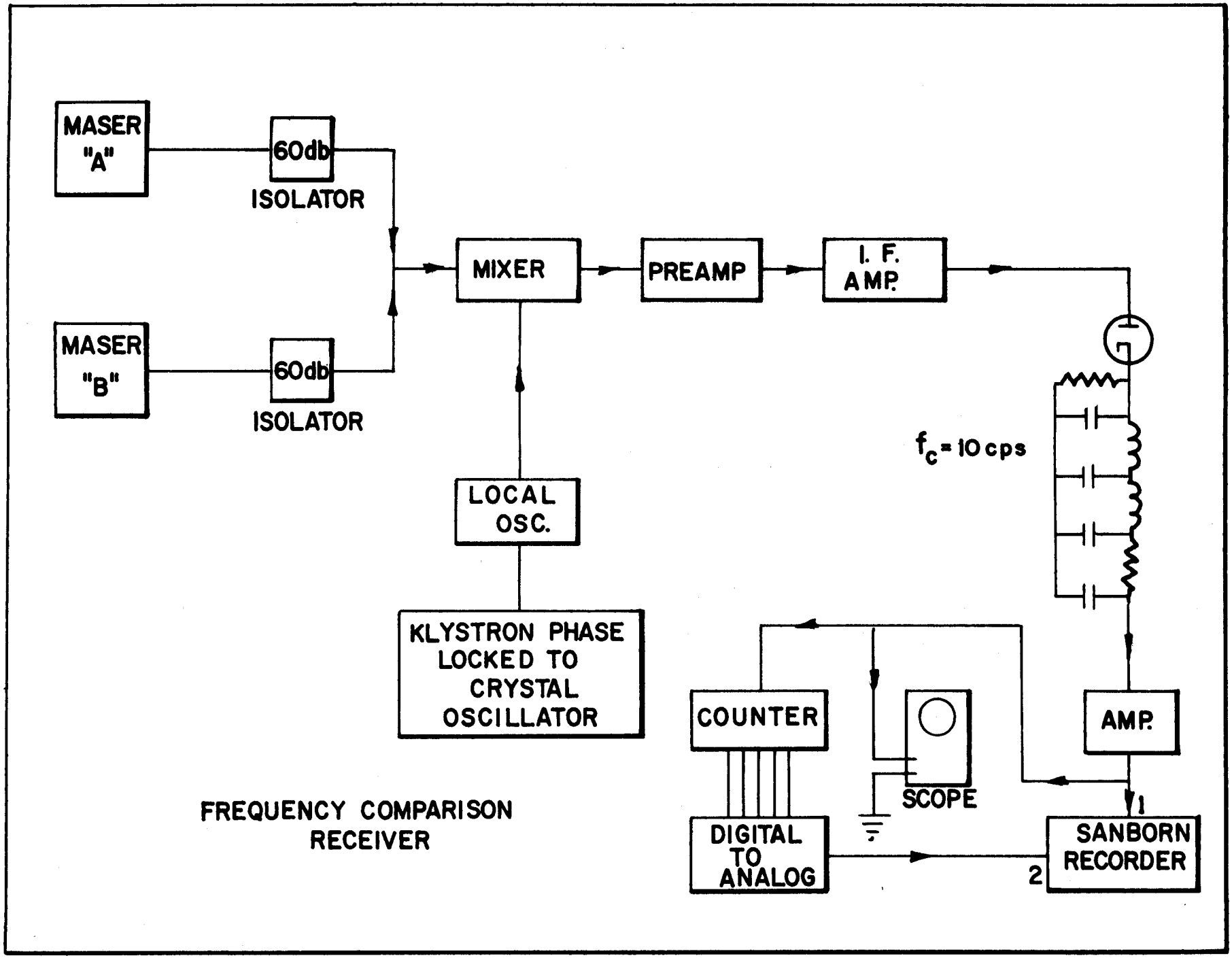
MASER "A"
60db
ISOLATOR
MASER "B"
60db
ISOLATOR
MIXER
PREAMP
I. F. AMP.
LOCAL OSC.
KLYSTRON PHASE LOCKED TO CRYSTAL OSCILLATOR
f_c = 10 cps
COUNTER
SCOPE
AMP.
DIGITAL TO ANALOG
SANBORN RECORDER
1
2
FREQUENCY COMPARISON RECEIVER

Figure 18

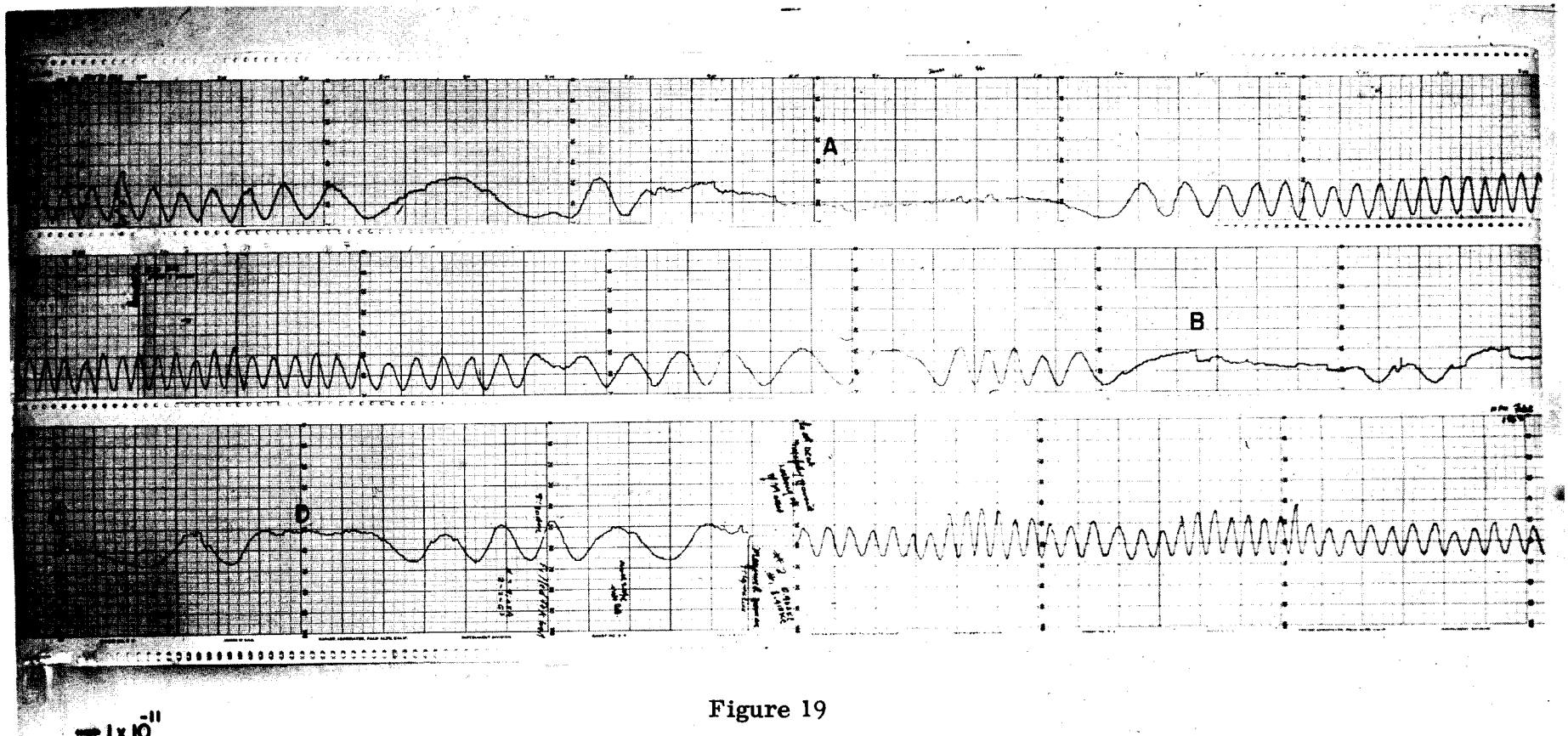

Figure 19

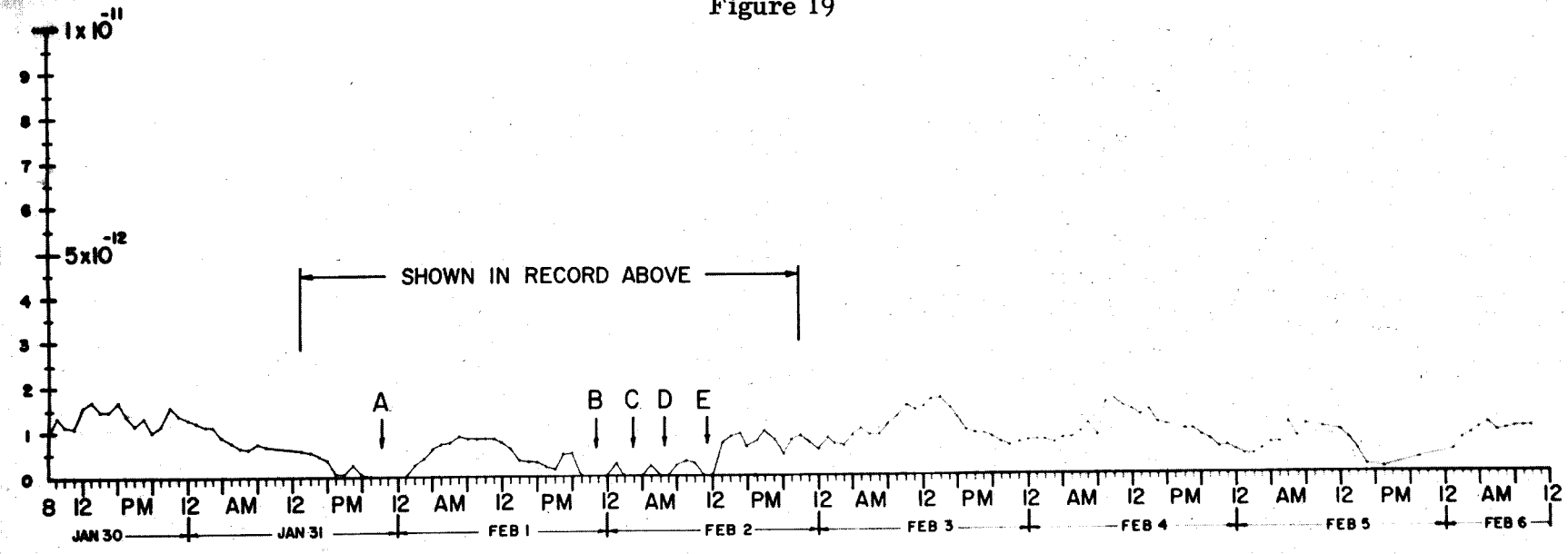

Figure 20

HOURLY DATA

68 CONSECUTIVE MEASUREMENTS

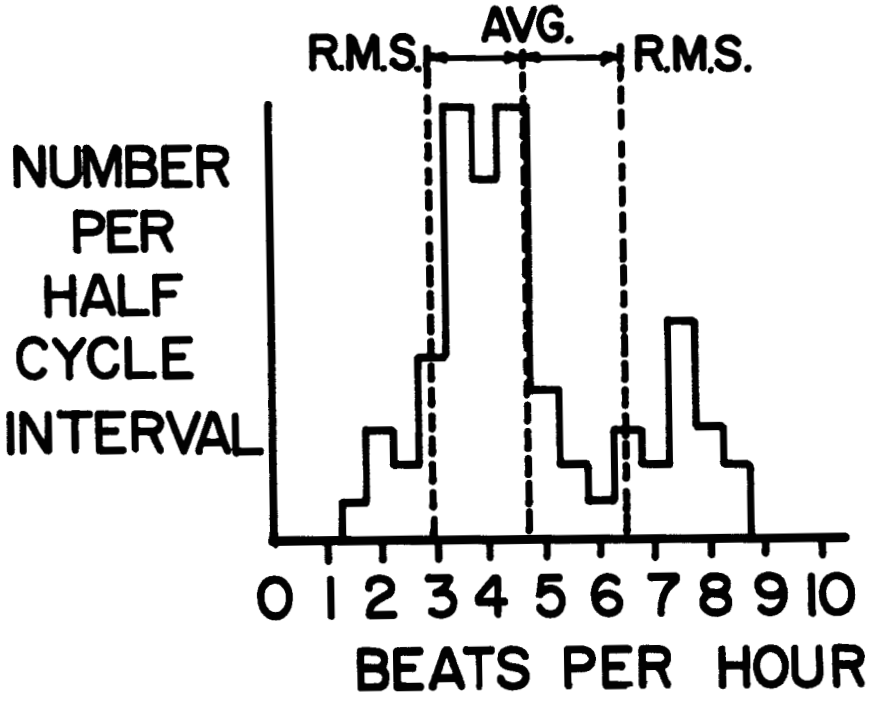

AVERAGE = 4.70 BEATS/HR.

R.M.S. DEV^{n} = 1.76 BEATS/HR.

$$\left.\frac{\langle \Delta f_{1\to 2}^{2} \rangle^{\frac{1}{2}}}{f}\right|_{1\,HR.} = 3.4 \times 10^{-13}$$

RMS FRACTIONAL FREQ. DEV^{n} FOR ONE MASER

$$\left.\frac{\langle \Delta f_{1}^{2} \rangle^{\frac{1}{2}}}{f}\right|_{1\,HR} = 2.4 \times 10^{-13}$$

Figure 21

10 SECOND PERIOD MEASUREMENTS OF FREQUENCY DEVIATION BETWEEN TWO MASERS

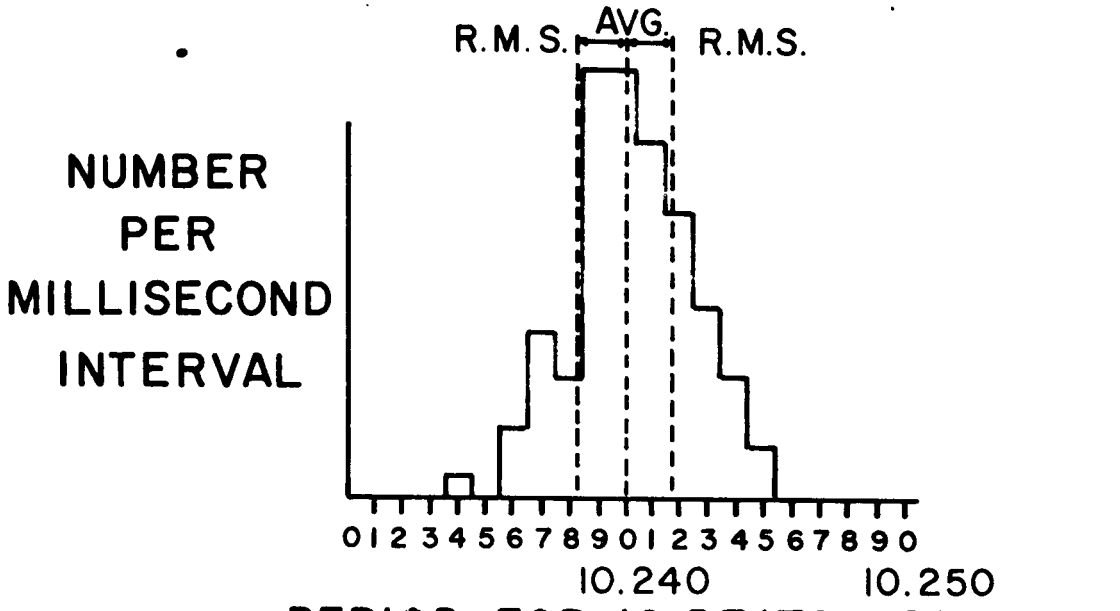

AVERAGE PERIOD = 10.2403 SECONDS

R.M.S. DEV^{n} = 1.86 MILLISECONDS

$$\frac{\langle \Delta f_{1-2}^2 \rangle^{\frac{1}{2}}}{f} = \frac{10}{f} \frac{\langle \Delta T^2 \rangle^{\frac{1}{2}}}{T_{AVG.}^2} = 1.24 \times 10^{-13}$$

R.M.S. FRACTIONAL FREQUENCY DEV^{n} FOR ONE MASER

$$\left. \frac{\langle \Delta f_1^2 \rangle^{\frac{1}{2}}}{f} \right|_{10\ SEC.} = 8.7 \times 10^{-14}$$

Figure 22.

magnetic effect, as the latter has not been observed and the correlation with room temperature is quite good. The greatest excursion in the beat frequency is 2.2×10^{-3} c.p.s. and corresponds to a relative fractional shift of 1.6×10^{-12}. The fractional r.m.s. deviation over one-hour intervals is 3.4×10^{-13} and if the fluctuations are uncorrelated, the r.m.s. fractional deviation for one maser is 2.4×10^{-13}.

Measurements of short term stability have been made using the previously mentioned method of offsetting the field to obtain a 1 c.p.s. beat frequency. The histogram for 94 measurements of the period for 10 beats to elapse is shown in Figure 22. The r.m.s. deviation for one maser is 8.7×10^{-4}.

Further data has been taken in a run that began April 9 and continues to this writing. Figure 23 shows the hourly measurement of frequency difference between the masers for 69 continuous days. The standard deviation of these hourly measurements is 4.8×10^{-13}. Closer inspection of the data will reveal an almost regular diurnal shift which correlates closely with temperature. On May 12-13 there is a very pronounced rise in the beat rate due to a drop in lab temperature from the normal 75° to below 60°F. Measured changes of the magnetic field at the bulb during some of these fluctuations have not been sufficient to cause these effects. On April 27-28 it will be seen that the beat increased suddenly. This was caused by the installation of three unshielded isolators having strong magnets while we were experimenting with the system. These were removed and the beat returned to normal.

It became apparent that some check on these measurements using outside standards was needed, as well as a measurement of frequency against the A_1 scale based on cesium taking the hyperfine frequency extrapolated to zero field as 9,192,631,770.00. A program of measurements via Loran "C" and V.L.F. was proposed by Markowitz and Hastings involving our monitoring the Loran transmitter on Nantucket Island and the V.L.F. at Cutler, Maine, and reporting the data to the Naval Observatory.

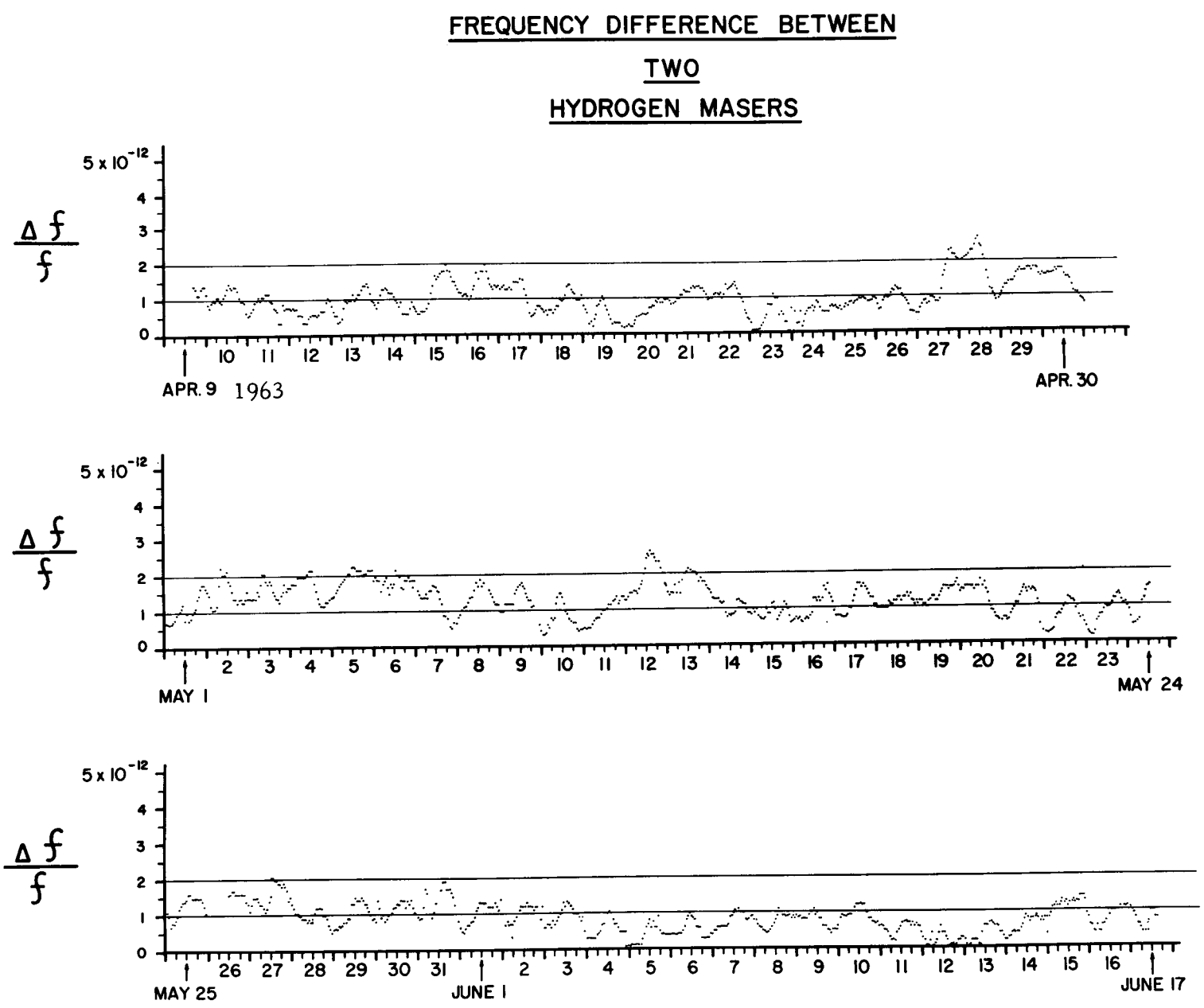
FREQUENCY DIFFERENCE BETWEEN
TWO
HYDROGEN MASERS
Δf/f
5 x 10⁻¹²
4
3
2
1
0
10 11 12 13 14 15 16 17 18 19 20 21 22 23 24 25 26 27 28 29
APR. 9 1963
APR. 30
Δf/f
5 x 10⁻¹²
4
3
2
1
0
2 3 4 5 6 7 8 9 10 11 12 13 14 15 16 17 18 19 20 21 22 23
MAY 1
MAY 24
Δf/f
5 x 10⁻¹²
4
3
2
1
0
26 27 28 29 30 31 2 3 4 5 6 7 8 9 10 11 12 13 14 15 16
MAY 25
JUNE 1
JUNE 17

Figure 23

TIME COMPARISON SYSTEM

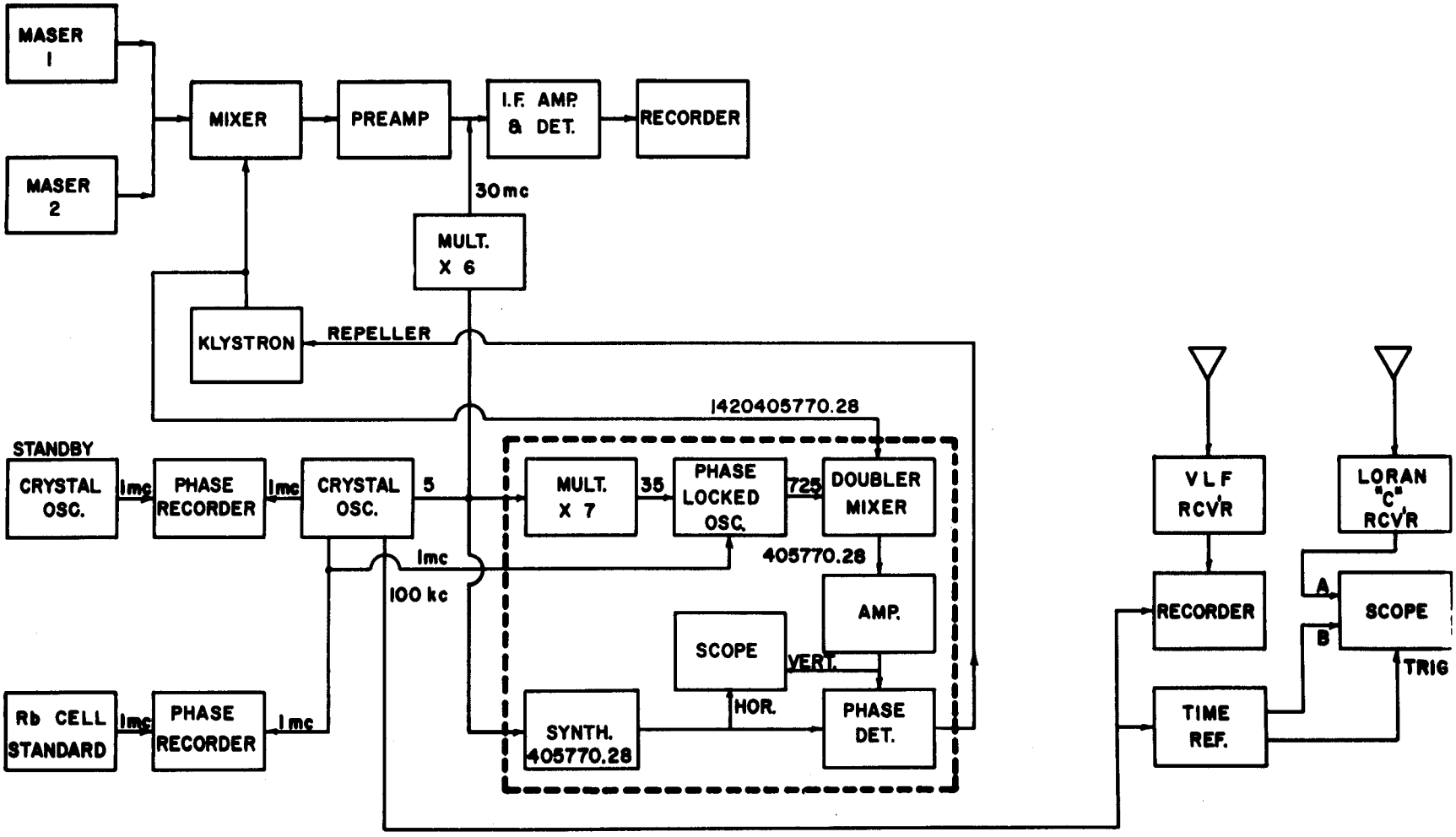

Figure 24

The problem of relating the hydrogen frequency to the Loran and V. L. F. that operate on the UT_2 time scale was solved in the following manner shown in Figure 24.

A klystron reference oscillator was phase locked to a 5 mc. crystal oscillator by using a phase locked signal at 1450 mc/sec derived from the crystal as a reference.

The klystron frequency of 1450 405 770.23 is obtained from a second phase lock using an offset of 405 770.23 c.p.s. derived from the same crystal using the Naval Research Laboratories' eight-digit synthesizer. Beats between the maser and the klystron occur at 30.000 000 03 mc/sec and are amplified and mixed with 30 mc from the crystal to give .03 c.p.s. beats that are described on a strip chart recorder. In this experiment some power from the second maser was introduced to give information of the relative maser stability. Figure 25 shows a one hour sample of these beats. The envelope describes the beats between the masers, and the more frequent beats between the stronger maser signal and the crystal oscillator can be seen.

Data was taken from May 9 to May 25 with about 2 $^1/_2$ days lost because of electronic problems at our lab and at the Loran site. The beats were counted and recorded with the Loran readings, and Figure 26 shows time measurements between the hydrogen masers and the Loran "C" taking an assumed frequency for hydrogen of 1420 405 770.200. The measurements can be made to better than one tenth of a microsecond accuracy, and over one day the spread between the readings is less than one microsecond. It should be noted here that the Loran station on Nantucket is slaved to a station on Cape Fear which operates from a Varian rubidium standard and that the total discrepancy seen here is due to the differences between the rubidium and hydrogen as well as the transmissions of the Loran from Cape Fear to Nantucket as well as from Nantucket to the laboratory in Beverly, Massachusetts.

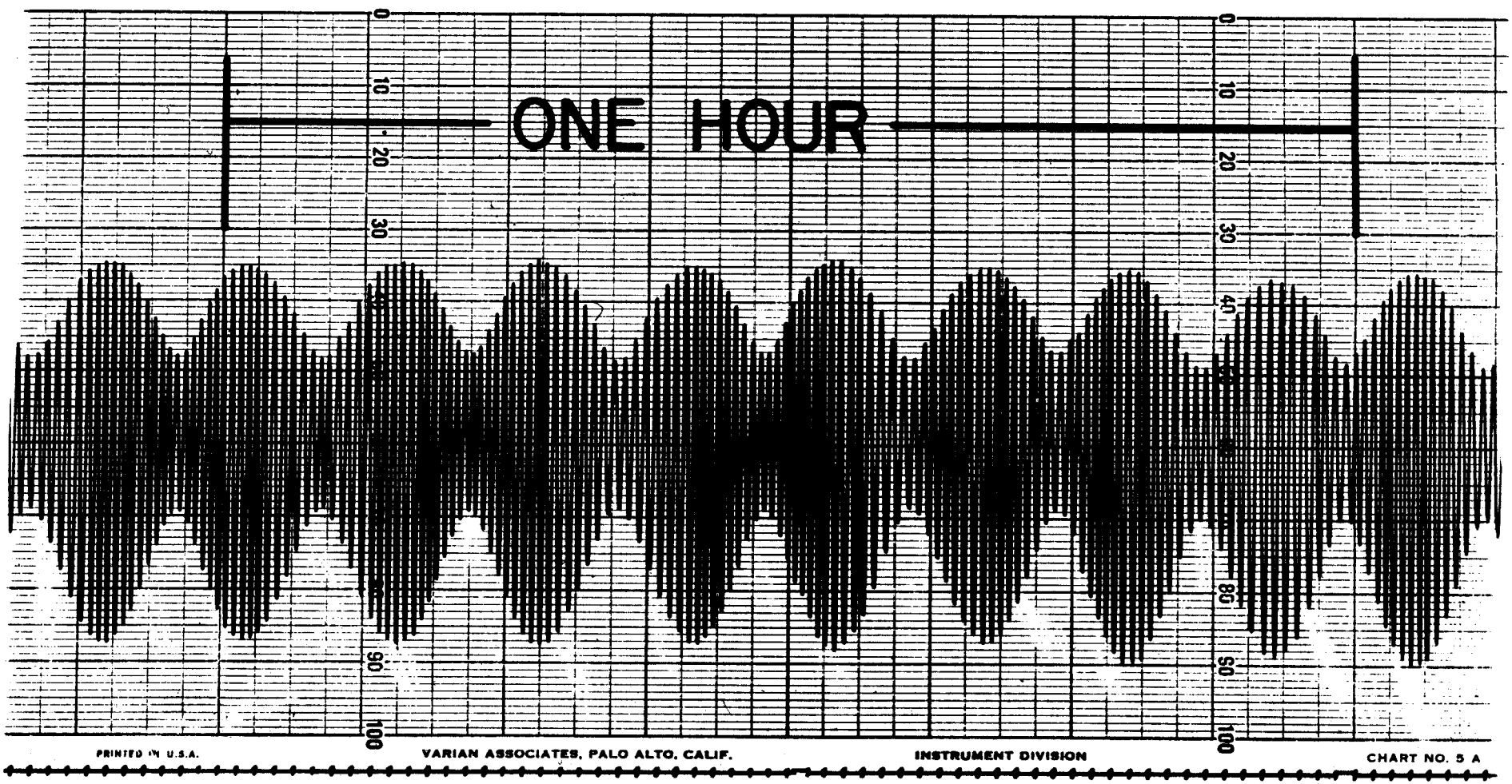
ONE HOUR
0
10
20
30
40
50
60
70
80
90
100
PRINTED IN U.S.A.
VARIAN ASSOCIATES, PALO ALTO, CALIF.
INSTRUMENT DIVISION
CHART NO. 5 A

Figure 25

LORAN "C" VS. HYDROGEN MASERS

BASED ON f_H = 1,420,405,770.200 cps

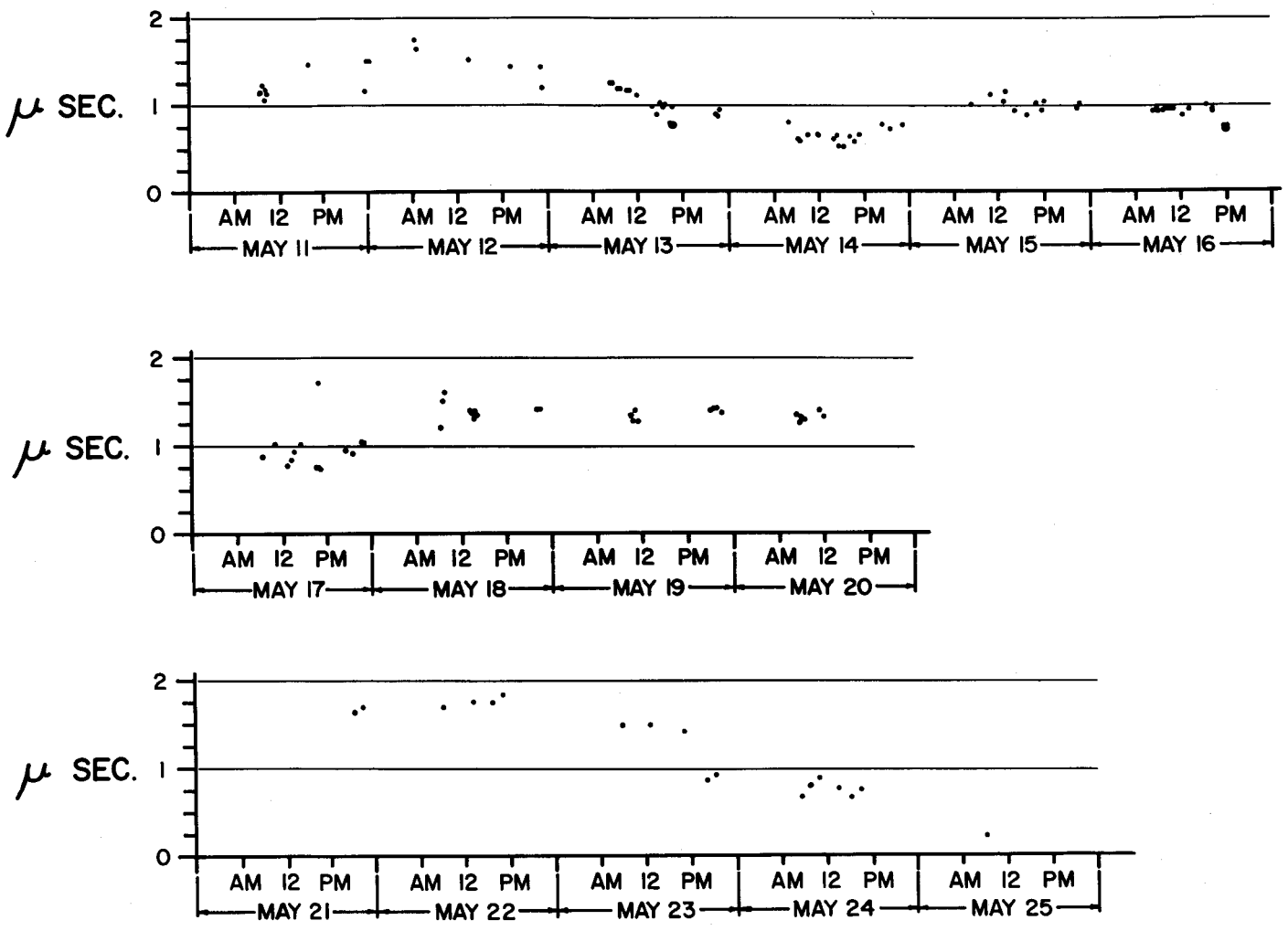

Figure 26

A change of one microsecond in four days represents a change of 2.9 parts in 10^{12}.

Over the whole run of May 9 -May 23, no over-all drift was seen and the maser was observed to be constant to within a few parts in 10^{12}.

3.2.4 Locking

In Figure 19 it can be observed that in those portions of the data where the beat frequency approaches 3×10^{-4} cycles per second there occurred a strong tendency to lock together. If power is transferred from one maser to the other, locking can occur when the power introduced is in the proper phase and of sufficient amplitude. The relation of the amplitude to the frequency difference for locking to occur is given by the expression relating the response of the atoms to a stimulating field

$$P = \frac{1}{2} I h \nu \frac{\langle x \rangle^2}{\gamma^2 + \langle x \rangle^2 + (\omega - \omega_o)^2}$$

where $\langle x \rangle^2 = \left[\frac{\mu_o}{\hbar} \right] \langle H_{zb} \rangle^2$ $\langle H_{zb} \rangle^2$ is average strength of the r.f. field in the bulb

For a small amount of power coupled into a maser , locking will occur when

$$\frac{P_{coupled}}{P} \geq \frac{\Delta\omega^2}{\gamma^2 + \langle x \rangle^2}$$

For two masers isolated by 60 db and operating under conditions where $\gamma = 1$ and $\langle x \rangle^2 \doteq 1$,

$$\Delta f = 2.2 \times 10^{-4} \text{ c.p.s.}$$

3.2.5 Effects of External Noise

In the expression for the r.m.s. fractional deviation given above, the effect of noise in a detection system has not been included. Receiver noise will degrade the observed signals especially if the observation time is short. (T_{obs} must, however, be larger than $\frac{1}{\gamma}$ or the expression is not valid.)

The maser fractional r.m.s. frequency stability over a time interval T_{obs} can be described as the angular fluctuation of a phase vector consisting of an amplitude vector rotating uniformly at angular frequency ω_o and a vector in quadrature to it having length

$$2 \times 0.113 \sqrt{\gamma^2 k T T_{obs}}.$$

The angular fluctuation

$$\langle \Delta \theta \rangle^{\frac{1}{2}} = 0.113 \times 2\gamma \sqrt{\frac{k T T_{obs}}{P_b}} .$$

The composite system of maser and receiver is described by a vector representing the amplitude available to the receiver rotating uniformly at ω_o having in quadrature with it a vector representing the root of the sum of the squares of the maser noise and receiver noise.

$$\langle \Delta \theta_{total}^2 \rangle^{\frac{1}{2}} = \sqrt{\frac{4 \times (0.113)^2 \gamma^2 k T T_{obs} + N k T B}{\frac{Q_{c,\ell}}{Q_{ext}} P_b}}$$

where B is the receiver bandwidth

$Q_{c,\ell}$ is the Q of the loaded cavity

Q_{ext} is the external Q of the cavity.

Regrouping the terms and rewriting this expression in terms of $\frac{\langle \Delta f^2 \rangle^{\frac{1}{2}}}{f}$,

$$\frac{\langle \Delta f^2 \rangle^{\frac{1}{2}}}{f} = \frac{0.113}{Q_\ell} \sqrt{\frac{k T}{P_b T_{obs}} \left[1 + \frac{19.5 N B}{\gamma^2 T_{obs}} \right] \frac{Q_{ext}}{Q_{c,\ell}}} .$$

Under the conditions that existed during the measurements, namely $N = 10$, $B = 10$ c.p.s., $\gamma = 0.7$ sec.$^{-1}$, $T = 300^{\circ}K$, $\frac{Q_{c,\ell}}{Q_{ext}} = 0.18$, $Q_{c,\ell} = 1.2 \times 10^9$, $P_b = 10^{-5}$ erg/sec, then

$$\frac{\langle \Delta f^2 \rangle^{\frac{1}{2}}}{f}\Big|_{1 \text{ sec.}} \doteq 9 \times 10^{-13}; \quad \frac{\langle \Delta f^2 \rangle^{\frac{1}{2}}}{f}\Big|_{10 \text{ sec.}} \doteq 7 \times 10^{-14}; \quad \frac{\langle \Delta f^2 \rangle^{\frac{1}{2}}}{f}\Big|_{1 \text{ hr.}} \doteq 1.4 \times 10^{-14}.$$

4.0 WORK IN PROGRESS

Once the work of developing and constructing the two state-of-the-art masers was completed and the masers were ready for delivery, an extension to the original contract was awarded to Varian by NASA to conduct experiments and make improvements under the following headings.

1. Conduct a measurement program for long and short term stability using three hydrogen masers.

2. Conduct measurements to determine the precision to which a given pair of masers can be reset with respect to frequency.

3. Conduct measurements to determine very short term relative stability. Very short term is defined as 0.01 seconds or less.

4. Measure the ratio of cesium to hydrogen frequencies of hyperfine separation.

5. Compare the two NASA masers with those at Harvard University.

The testing of long term stability has been in progress for some time and has been discussed in the previous sections. From the data obtained, one can observe several obvious places to make improvements. The diurnal variations are due to temperature changes in the lab and the effect of these changes on the cavity tuning. Temperature compensation of the cavity should be improved as well as the means for controlling the temperature itself. A further improvement to this would be to redesign the resonator to take advantage of the solid dielectric cavity idea wherein a spherical, heavy-walled vessel is used as both a storage bulb and a resonator. The heavy dielectric wall would produce a resonator resonant at 1420 mc/sec., having an 8" outside quartz sphere with an inner recess about 5" in diameter.

Besides the reduction in size, considerable gain in ruggedness and stability is available with this configuration. There is also the advantage that spherical, hence isotropic magnetic shields can be used. A set of orthogonal magnetic windings having a sinusoidal density will provide exactly the uniform magnetic

field needed in the bulb. Work along these lines is in progress and the calculation of the exact dimensions is being set up on a high speed computer.

Further improvements in the gas handling system are needed to afford a large range of flux control. One of the first limitations found in the cavity tuning technique involving the variation in the beam flux was found to lie in the control of hydrogen flux to the discharge. The controlling element is a mechanical leak which leads to a palladium tube purifier and then to the discharge. Mechanical leaks have been found to be critical to adjust and just about impossible to reset to a given value. The palladium tube, however, offers a measure of flux control because of the temperature dependence of the solubility of hydrogen in this metal.

Unfortunately, because of the desirability of keeping the discharge system clean, the palladium tube is the last component in the line and acts analogously to a variable resistor across a condenser representing the reservoir about the palladium purifier.

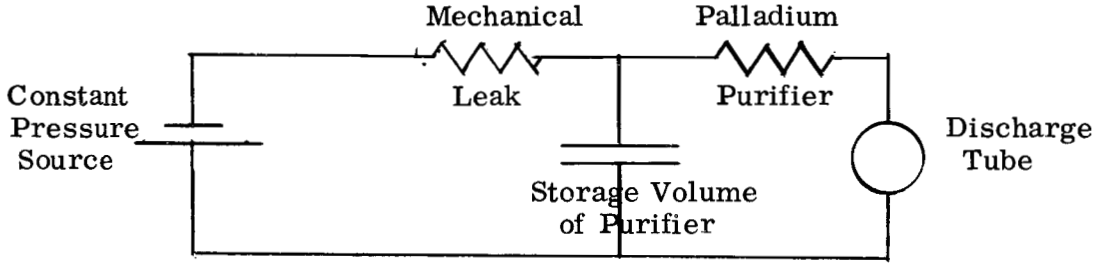

Electrical Analog of Pressure Control

The pressure excursions are limited and it is very difficult to maintain high or low flow to the source. Nevertheless, the tuning has been done and after several trials, the relative resettability of the maser is found to be about 1 in 10^{12}.

Improvements in this measurement will certainly be obtained with the installation of a better flow control and this system is now under construction.

Further beat measurements are being made and, with the help of an 8-channel recorder, the data is being correlated with other parameters such as source pressure, vacuum pump current, room temperature, room magnetic field, S cavity temperature, etc. The effort is directed to determine the causes of instability and, if possible, find ways to eliminate them.

5.0 REVIEW OF IDEAS AND INVENTIONS

Patent disclosures have been written on the work done for NASA under the following headings:

1. Temperature Compensated Maser Cavity
2. Vacuum Enclosed Cavity
3. Thermocouple Servo Neck Control
4. Solid State R.F. Hydrogen Dissociator

These topics represent ideas that were either conceived or reduced to practice while working on the NASA contract. Other innovations and new techniques that have come to light during this contract are described briefly below.

a) A common shielded enclosure for both VacIon pumps;

b) A mounting scheme for the hexapole eliminating a flanged joint near the source;

c) The use of a ferromagnetic septum in the vacuum system to help shield field gradients from the hexapole;

d) The use of a captive "O" ring joint at the base of the bell jar instead of welding it closed;

e) The development of chopper stabilized d.c. amplifiers for use in controlling the neck, and inner and outer oven temperatures.

6.0 REVIEW OF PAPERS AND PUBLICATIONS

"Design and Performance of an Atomic Hydrogen Maser," R.F.C. Vessot and H.E. Peters, International Conference on Precision Electromagnetic Measurements, Boulder, Colorado, August 16, 1962. (IRE Trans. on Instrumentation, Vol. I-11, Nos.3,4, Dec.1962.)

"Frequency Stability Measurements Between Several Hydrogen Masers," R.F.C. Vessot, Third Internation Symposium on Quantum Electronics, Paris, France, February 11, 1963. (Paper to appear in Proceedings.)

"Frequency Beat Experiments with Hydrogen Masers," R.F.C. Vessot and H.E. Peters, 17th Annual Symposium on Frequency Control, Atlantic City, New Jersey, May 27, 1963. (Frequency Magazine, Vol.6, p.28, Sept.-Oct. 1963.)

Talks by R.F.C. Vessot:

U.S.Navy R&D Symposium, Columbus, Ohio, June 11, 1963;

U.S. Naval Observatory, May 2, 1963;

University of Rochester, January 1963;

National Research Council of Canada, December 5, 1963.

REFERENCES

1. O. Stern, Zeits.f. Physik 7, 249 (1921).
2. Gerlach and O. Stern, Ann. Physik 74, 673 (1924).
3. I. I. Rabi, J.R. Zacharias, S. Millman and P. Kusch, Phys.Rev. 53, 318 (1939).
4. J.M.B. Kellogg, I.I. Rabi, N.F. Ramsey and J.R. Zacharias, Phys. Rev. 55, 728 (1939).
5. N.F. Ramsey, Phys. Rev. 76, 996 (1949).
6. N.F. Ramsey, Phys.Rev. 78, 695 (1950).
7. J. P. Gordon, H. J. Zeiger and C.H. Townes, Phys.Rev.95, 282 (1954).
8. J.P. Gordon, H. J. Zeiger and C. H. Townes, Phys.Rev.99, 1264 (1955).
9. D. Kleppner, N.F. Ramsey and P. Fjelstad, Phys.Rev. Letters I, 232 (1958).
10. H.M.Goldenberg, D. Kleppner, N.F. Ramsey, Phys.Rev.Letters V, 361 (1960).
11. H.M. Goldenberg, D. Kleppner, N.F. Ramsey, Phys.Rev. 123, 530 (1961).
12. R.W. Wood, Proc. Roy.Soc. 97, 455 (1920).
13. R.W. Wood, Proc. Roy.Soc. 102, 1 (1922).
14. D.E.Nagle, R.S. Julian and J.R. Zacharias, Phys.Rev. 72, 971 (1947).
15. L. Davis. T.F. Feld, C.W. Zabel and J.R. Zacharias, Phys.Rev. 76, 1068 (1949).
16. Basic Data of Plasma Physics, M.I.T. and Wiley (1959).
17. P. Warneck, Applied Optics 1, 721 (1962).
18. G. Bennewitz and W. Paul, Zeits.f. Physik 139, 489 (1954).
19. H. Friedberg and W. Paul, Naturwissenschaften 37, 20 (1950).
20. H. Friedberg and W. Paul, Naturwissenschaften 38, 159 (1951).
21. R.L. Christensen and D.R. Hamilton, Rev.Sci.Instr. 30, 356 (1959).
22. A. Lemonick, F.M. Pipkin and D.R. Hamilton, Rev.Sci.Instr. 26, 1112 (1955).
23. N.F.Ramsey, Molecular Beams, Oxford Univ.Press (1956)..pp.78, 84.
24. D. Kleppner, H.M. Goldenberg and N.F.Ramsey, Phys.Rev. 126, 603 (1962).
25. K. Shimoda, T.C. Wang and C.H. Townes, Phys.Rev. 102, 1308 (1956).
26. W.A. Edson, Proc.IRE 48, 1454 (1960).

REPORT ON THE FREQUENCY OF HYDROGEN

by Wm. Markowitz
U. S. Naval Observatory
24 May 1963

1. The hydrogen quantum transition is a possible choice for the definition of the atomic second. It is necessary that its frequency be determined with high precision with respect to the unit of time adopted by the International Committee of Weights and Measures, namely the second of ephemeris time. In practice, this second is obtained from the cesium beam, using an adopted frequency of 770 for the cesium transition at zero magnetic field.

2. ONR and NASA have sponsored research on the hydrogen maser of N. Ramsey. In May 1963, a determination of the frequency of hydrogen was carried out with hydrogen masers constructed under this program by Bomac Labs. The masers are located in Beverly, Mass. The instrumentation for the frequency comparison was supplied by the Naval Research Laboratory. The reference system of time is A. 1, derived by the U.S. Naval Observatory, Washington. The masers at Beverly were linked to the master clock at the Naval Observatory through common monitoring of the Loran-C stations at Nantucket and Cape Fear.

The system A. 1 is based on cesium beam oscillators at 8 laboratories which report the frequency of the VLF transmissions of NBA referred to their cesium oscillators. These are:

Table I: Cesium oscillators, with weights, used in forming A. 1

	Wt.		Wt.
N. O., Wash.	2	CNET, Paris	1
N. O., Rich.	2	NBS, Boulder	10
NRL, Wash.	2	NPL, Tedd.	10
Cruft	2	Neuchâtel	10

3. The frequency synthesizer settings, the beat counts, and Loran-C readings made at Beverly by Bomac were forwarded each day to the Naval Observatory.

A correction of -.0023 cps was applied to the observed frequency of hydrogen for the magnet shift. No other corrections to hydrogen were made. Figure 1 shows the frequencies obtained. Figure 1 also shows three sets of means. Line (a) gives the frequency of hydrogen with respect to the measuring system of the Naval Observatory. This was stable during these tests to a few parts in 10^{12}.

Line (b) gives the frequency with respect to cesium, which is considered to be reproducible over long time intervals to 1 part in 10^{11}. The uncertainty due to wall shift of hydrogen is not known and is not included in the probable error.

Line (c) gives the frequency with respect to the second of ephemeris time. Since this has been determined to 2 parts in 10^9 we round off to the last unit. It should be noted that if hydrogen is selected to define the atomic second, the value resulting from this experiment would be that given by line (c), but the definition would not contain a probable error.

4. Hydrogen may be used as a standard of frequency. Assuming that the frequency of hydrogen was 751.734 we may derive values of the frequency of Loran-C, controlled by the Naval Observatory. These are shown in Figure 2. The mean frequency was -129.98×10^{-10} with respect to A.1 and the probable error of a daily mean is 3×10^{-12}.

5. These experiments have related the frequency of a particular hydrogen maser to that of external standards located in laboratories several hundred and several thousand miles away through VLF and Loran-C. The stability of hydrogen, based on internal comparisons in the laboratory and on these external comparisons, appears to be very high. Nevertheless, additonal experiments must be made before we can say if hydrogen is superior to other quantum transitions for defining the atomic second.

Table II. Summary of Results

1963 Mean Epoch	Interval (weight)	Assuming Cs = ..770, ν_H = ..751.734+	Assuming ν_H = ..751.734, Loran-C = -130.00×10^{-10}+
	d		
May 12.3	1.4	+ 0.010 cps	$- 1 \times 10^{-12}$
13.4	0.6	- .006	+ 10
14.2	0.8	- .016	+ 8
15.0	1.0	+ .004	- 4
16.3	1.2	- .001	+ 6
18.1	1.5	- .004	- 4
19.3	0.6	- .002	+ 1
20.4	0.8	- .005	+ 3
22.5	0.8	+ .007	+ 4
23.4	1.0	+ .003	+ 5
		P.E. of unit wt. = ± 0.005 cps	P.E. of unit wt. = $\pm 3 \times 10^{-12}$

(a) 1 420 405 751.734 ± 0.002 cps

(b) 1 420 405 751.73 ± 0.02

(c) 1 420 405 752 ± 3

V_H ON A.I.

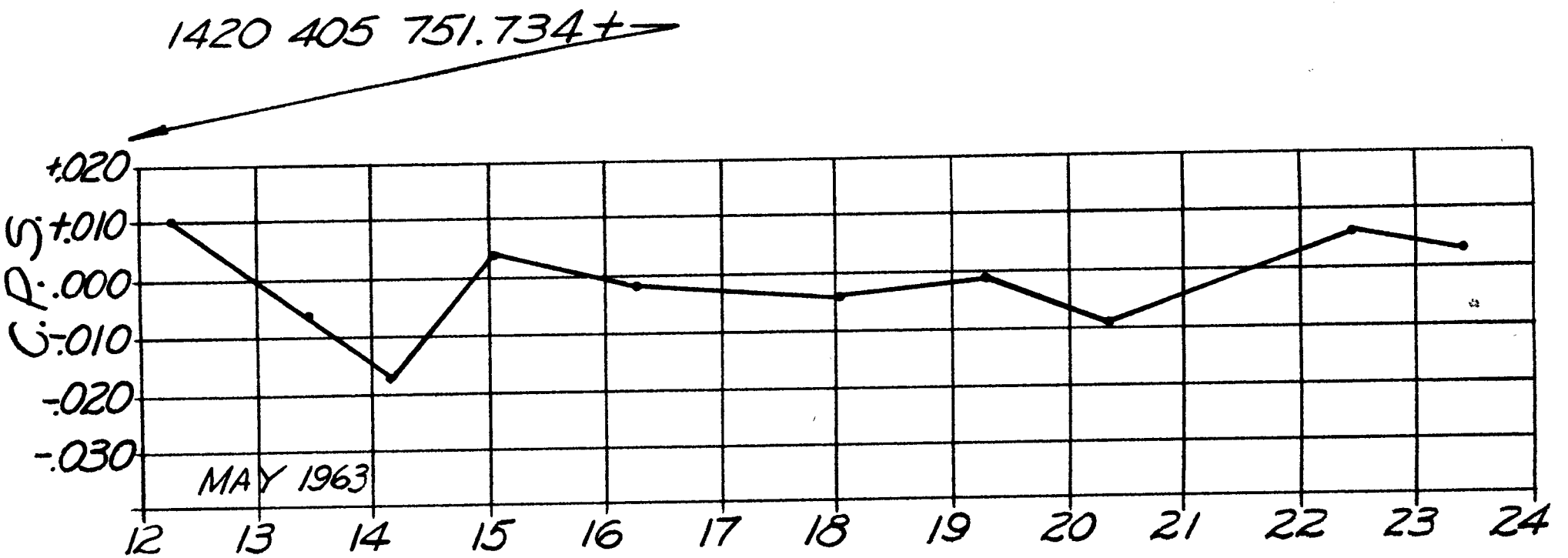

(a) 1420 405 751.734 ±.002 CPS (frequency system Nav Obsy. May 1963)
(b) 1420 405 751.73 ±.02 (cesium)
(c) 1420 405 752 ±3 (second of E.T.)

FIG. 1

LORAN-C FREQUENCY

ASSUMING ν_H = 1 420 405 751.734 CPS

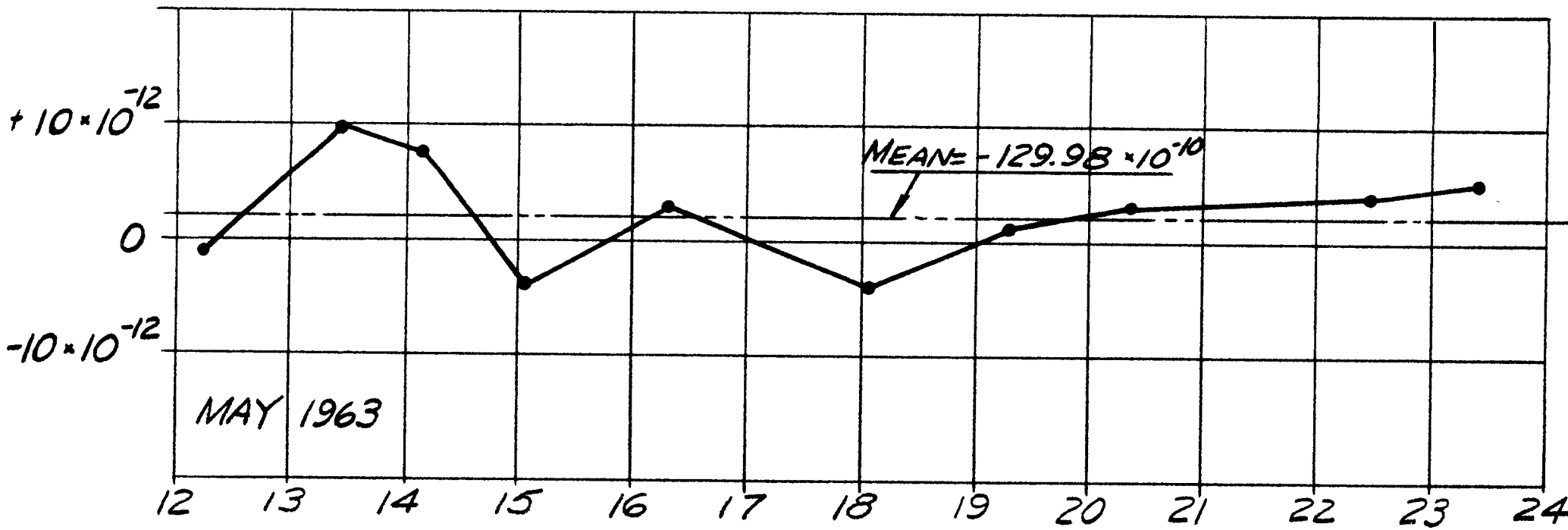

FIG. 2